The Characterization of the Molecular Structure and the Partners of MLIP

Fawaz Saleh, B.Sc.

University of Ottawa Heart Institute

Thesis submitted to the Faculty of Graduate and Postdoctoral Studies, in partial fulfillment of the requirements for M.Sc. degree in Cellular and Molecular Medicine

Department of Cellular and Molecular Medicine

Faculty of Medicine

University of Ottawa

1. Abstract

A novel gene, Muscle-enriched A-type Lamin-Interacting Protein (MLIP), was identified in our lab through a yeast two-hybrid screen using Lamin A/C N-terminal sequence as bait (10-230 amino acids), in an attempt to shed light on the complex nature of laminopathies. MLIP is a non-homologous, single copy gene conserved in amniotes. MLIP's expression differs between tissues and is subjected to extensive tissue-dependent alternative splicing. Some of MLIP's isoforms, lacking specific exons, have been identified and referred to as MLIP Δ2, Δ3, Δ4, Δ6, Δ8 and Δ10. The putative Lamin binding domain was identified to be within the first 41 amino acids of MLIP, spanning across exon 1 and 2 of the *MLIP* gene. MLIP's Molecular function remains largely unknown. The main **objective** of this study is to map the exact location of MLIP:Lamin A/C binding domain and the identification of MLIP isoform specific binding partners in different tissues. We **hypothesized** that the MLIP:Lamin binding domain is specific interaction and is located on the protein encoded by exon 1. We also hypothesized that the phenotypic observations in laminopathies may be in part due to the differential MLIP isoform expression in different tissue, whereas MLIP isoforms have different binding partners in different tissues resulting in variable functions. Our **results** demonstrate that MLIP is a spliced protein that contains alternative promoters that are tissue specific, which we annotated as MLIP-1a and 1b. The MLIP alternative promoters are located on the 5' end of the *MLIP* gene and contain an alternative start site situated on exon 3. We also found that MLIP-1a splice variants are predominantly expressed in the heart and skeletal muscle, whereas MLIP-1b splice variants are expressed in almost all

tissue types studied. In addition, hMLIP binds to Lamin A/C and the hMLIP-Lamin binding domain is exclusively specific to the protein encoded in exon-1a of the *MLIP* gene. Moreover, MLIP and it's splice variants (1a and 1b) show high levels of expression in the early post-natal heart which decrease with age, mimicking the expression of Lamin A/C. This gives us a good indication that MLIP:Lamin A/C interaction plays a vital role in heart development and mutations in that part of the gene might contribute to laminopathies pathology.

2. Acknowledgements:

I would like to extend my gratitude to the many people who helped to bring this research project to fruition. First, I would like to thank Professor Patrick G. Burgon for providing me the opportunity to pursue graduate studies. I am so deeply grateful for his help, professionalism, valuable guidance and financial support throughout this project and through my entire program of study that I do not have enough words to express my deep and sincere appreciation. I must extend a most grandiose thank you to the members of my thesis advisory committee, Dr. Balwant Tuana and Dr. Alexandre Stewart, for their constructive feedback, suggestions and direction. I would also like to extend a heartfelt thank you to Dr. Marie-Elodie Cattin, Esther Mak-Washburn, Cassandra Roeske, Jonathan Weldrick for their support over the course on my project.

Finally, I must express my very profound gratitude to my parents and family for providing me with unfailing support and continuous encouragement throughout my years of study and through the process of researching and writing this thesis. This accomplishment would not have been possible without them. Thank you.

3.List of Abbreviations

MLIP = Muscle enriched A-type Lamin interacting protein
LMNA = Lamin A gene/protein
IF = Intermediate Filaments
LMNB1 = Lamin B1 protein
LMNB2 = Lamin B2 protein
L1 = Linker region 1
L12 = Linker region 12
L2 = Linker region 2
DNA = Deoxyribonucleic acid
LMO7 = Lim domain Only Protein 7
PKM2 = Pyruvate Kinase Muscle Isozyme
cDNA = Complementary Deoxyribonucleic acid
IPTG = isopropyl-1 thio D-galactopyranoside
Rpm = Round per minutes
GST = Glutathione Sulphor Transferase
TnT = In-vitro Transcription Translation
RNA = Ribonucleic Acid
PCR = Polymerase Chain Reaction
SDS = Sodium Dodecyl Sulfate
SDS-PAGE = Sodium Dodecyl Sulfate Polyacrylamide Gel Electrophoresis
PBS = Phosphate Buffered Saline
TBST = Tris-Base tween-20
IP = Immunoprecipitation
kDa = KiloDalton
T1D = Type 1 Diabetes
SNP = Single Nucleotide Polymorphism
EF = Elution Fraction
GST = Glutathione Sulphor Transferase

4. List of Figures and Tables

Figures in thesis copyrighted with permission from publishers

Figure 1: this figure is reprinted by permission from Physiology Review Broers JL, Ramaekers FC, Bonne G, Yaou RB, Hutchison CJ. Nuclear lamins: Laminopathies and their role in premature ageing. 2006.

Figure 3: This figure is printed by permission from Biochemical Society Transactions: Bertrand A., Chikhaoui K., Yaou R.B. and Bonne G. Clinical and Genetic Heterogenity in laminopathioes. Biochemicals transactions 2011

Figure 4: This figure is printed by permission from Journal of Biological Chemistry: Ahmady E, Deeke SA, Rabaa S, Kouri L, Kenney L, Stewart AFR, Burgon PG. Identification of a Novel Muscle A-type Lamin-interacting Protein (MLIP). 2011

Table 1: Permission granted, Adapted from Capell al. et nature Genetics 2006.

Table 2: Permission granted by CC-BY licence, Röber RA, Weber K, Osborn M. Differential timing of nuclear lamin A/C expression in the various organs of the mouse embryo and the young animal: a developmental study. Development. 1989 Feb

Table of Contents

Chapter 1:

Introduction, Hypothesis, Rationale and Objective of Proposed Study

5. Introduction:

5.1 Nuclear Envelope and Lamina

The nucleus is surrounded by the nuclear envelope that separates nuclear contents from the cytoplasm. The nuclear envelope consists of an inner and an outer membrane separated by peri-nuclear space, and connected at nuclear pores. Nuclear pores play a key role in regulating the transport of materials such as RNA and protein between the nucleus and cytoplasm (Gerace *et al.,* 1978).

Nuclear lamins are a type of intermediate filament (IF) proteins that comprise an integral part of the nuclear lamina. The IF super-family consists of 60 members, belonging to 5 different groups (I-V). Most IF super-family proteins are cytoplasmic (from I-IV), while lamins, which belong to group V, are nuclear. Lamins are not only found in the nuclear lamina, but also in the nucleoplasm (Hutchinson *et al*, 2002).

5.2 Type of Lamins and their structure

There are two types of lamins, A-type lamins and B-type lamins. The A-type lamins are further sub-divided into two splice isoforms, A and C, which are derived from different splicing and alternative polyadenylation of the *LMNA* gene. B-type lamins are also divided into two sub-types, B1 and B2 lamins, which are encoded by two separate genes, *LMNB1* and *LMNB2*. Both A-type and B-type lamins are constituents of the nuclear lamina (Genschel and Schmidt, 2000), and the B-type lamins are expressed at constant levels in all multicellular eukaryotic cells (Stuurman *et al*., 1998).

Nuclear lamins contain a variable NH_2-terminal globular head domain, a ∝-helical rod comprising four coiled-coil domains separated by linker regions L1, L12 and L2 and a globular COOH-terminal tail domain that contains a nuclear localization signal (NLS). The coiled-coil domains form rope-like structures, and in lamins these domains form dimers, the coiled-coil domains 1A, 1B, 2A and 2B are organized around heptad repeats (Figure 1) (Quinlan *et al*. 1985) (Conway *et al* 1990).

5.3 Function of Lamins

The nuclear lamina predominantly lies under the inner nuclear membrane. Its fundamental role is to provide structural support for the nucleus. Lamins also regulate nuclear envelope (NE) organization by anchoring and spacing nuclear pore complexes (NPCs). Lamins interact with NPCs in the early stages of lamina assembly and are involved in proper NPC localization. The lamina also plays a role in a variety of cellular processes, such as chromatin organization, transcription and mitosis; therefore the nuclear lamin interacts with DNA, chromatin, transcription factors and proteins from the inner nuclear membrane (Moir *et al*., 2000).

5.4 Lamin A/C

In mammals, the two major isoforms of A-type lamins are lamin A (70 kDa) and lamin C (60 kDa). The *LMNA* gene in humans contains 12 exons and alternative splicing at exon 10 allows for the generation of lamin A and C. Lamin A and C share the first 566 amino acids, Lamin A has an additional 98 amino acids and Lamin C has

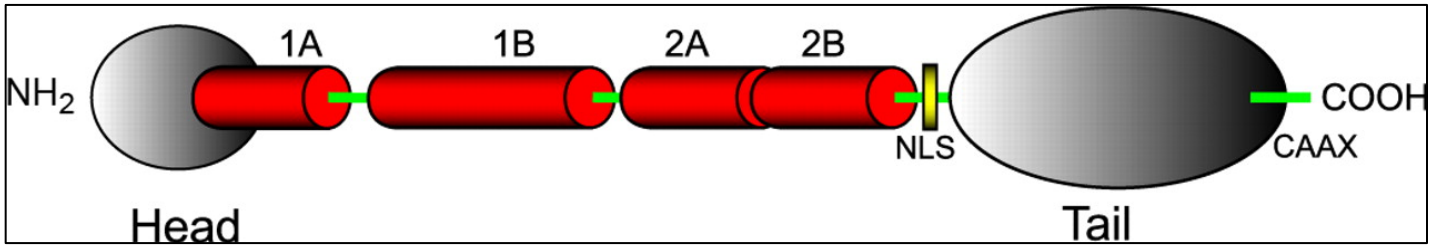

Figure 1: Schematic representation of the structure of lamin proteins. Lamin proteins consist of a N-terminal globular head domain and a C-terminal globular tail domain that flank the central rod domain, comprising four coiled-coil domains 1A, 1B, 2A and 2B. The globular tail domain consists of the nuclear localization signal (NLS) and CAAX motif (found in lamin A and lamin B, but not in lamin C) **(Broers et al., 2006)**

an additional 6 amino acids. The expression of A-type lamins is more developmentally regulated. The expression of A-type lamins increases during differentiation and is highest in terminally differentiated cells (Machiels *et al*., 1996).

While lamin A and C share the first 566 amino acids, lamin C lacks exon 11, and exon 12. Instead it carries 5 lamin C-specific amino acids before early termination. Lamin A, on the other hand, carries a lamin A specific region from amino acid 566-664 (Broers, *et al*., 2006).

The carboxyl terminus of pre-lamin A and B contains a CAAX box (Cysteine-aliphatic-aliphatic-any residue), which is absent in lamin C. For conversion to lamin A, pre-lamin A is modified by iso-prenylation (farsenylation) of the cysteine residue, followed by removal of the AAX sequence by ZMPSTE24 protease (Zastrow *et al*., 2004). Subsequently, the COOH-terminal cysteine residue undergoes carboxymethylation. Both these processes are important for localization of lamins to the inner nuclear membrane (Broers *et al*., 2006).

5.5 Laminopathies: LMNA mutations and diseases

Laminopathies are a group of genetic disorders caused by mutations in genes encoding proteins of the nuclear lamina. Over 500 different mutations have been identified to occur in lamins and these kinds of mutations can lead to the development of over fifteen different laminopathies (Genschel and Schmidt, 2000) (Figure 2). The different tissues affected by mutations in the LMNA gene that result in lamiopathies, display no genotype and phenotype correlation which indicates the

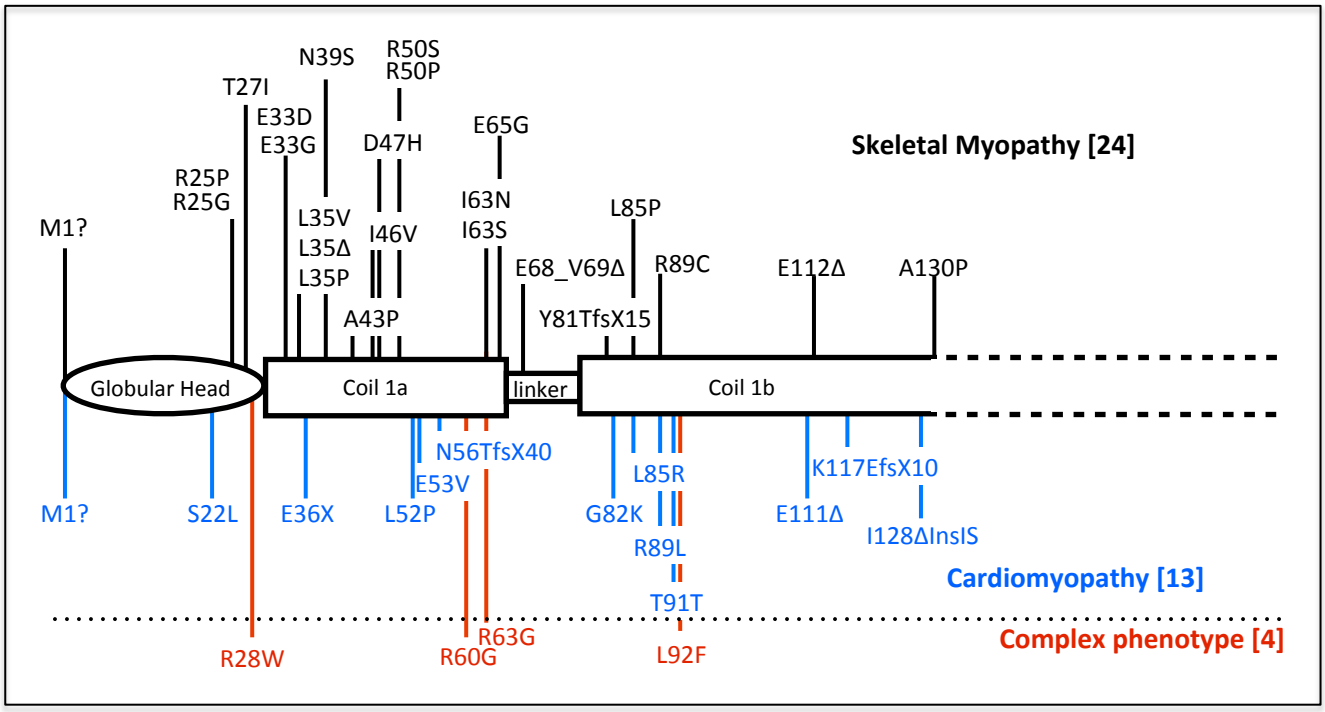

<u>Figure 2</u>: Mutation in human LMNA that are associated with skeletal and cardiac Myopathies as well complex phenotype; which is a combination of skeletal and cardiac myopathies. The schematic diagram displays the nomenclature of the mutations located on the Lamin A/C protein, the mutation denoted in black, blue and red show missense mutations where the first letter represents the original amino acid and its location and the second letter shows the amino acid that it was changed to.

mechanisms governing those mutations are largely unknown (Genschel and Schmidt, 2000) (Figure 3). These conditions can be divided into several categories based on the symptoms and how they affect the human body. Within the first category are the diseases that cause progeria, also known as premature aging. In the second category are the diseases that cause peripheral neuropathy while the third category includes diseases that result in partial lipodystrophy. The forth and final category comprises the diseases in which striated muscle is effected (Genschel and Schmidt, 2000). The phenotypes of these diseases are summarized in Table 1 and Figure 3.

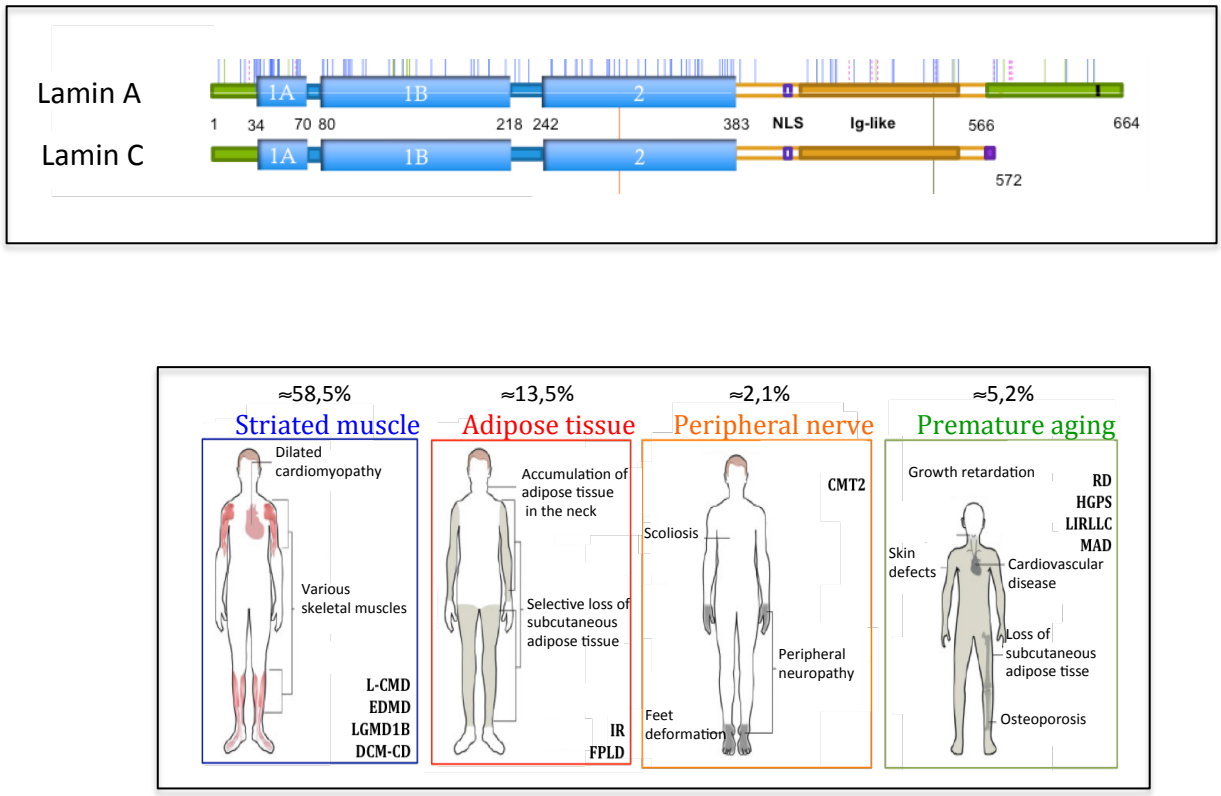

Figure 3: Lamaniopathies Phenotype and Genotype Correlation: Mutations in lamin A/C give rise to a group of heterogenous genetic disorders, which display a large variety of complex clinical entities including Striated muscle (Blue) which accounts for 58.5% of total mutations, which resembles the blue lines shown in the gene (LMNA-related congenital muscular dystrophy, Emery Dreifuss muscular dystrophy, Limb-Girdle Muscular dystrophy and Dialated Cardiomyopathy with conduction defects), Adipose tissue 13.5%, which resembles the red lines in the gene (Insulin Resistance Syndrome and Familial partial lipodystrophy), Peripheral nerve 2.1%, which resembles the yellow line in the gene. (Charcot-Marie Tooth Syndrome) and Premature aging 5.2%, which resembles the green line in the gene (Restrictive Dermopathy, Hutchinson-Gilford progeria syndrome). The different mutations that occur in the LMNA gene (over 400 different mutations) have no genotype and phenotype correlation. This figure is printed by permission from Biochemical Society Transactions: Bertrand A., Chikhaoui K., Yaou R.B. and Bonne G. Clinical and Genetic Heterogenity in laminopathioes. Biochemicals transactions 2011.

Table 1: Mutations in *LMNA* lead to a variety of human degenerative disorders, collectively termed laminopathies. The table presents various laminopathies with their modes of inheritance, clinical phenotypes and primary LMNA domains in which mutations are found. (Adapted from Capell *et al* Nature Genetics 2006).

Disease	Category	Form of inheritance	Clinical phenotype
Emery-Dreifuss Muscular dystrophy (EDMD)	Striated Muscle	Autosomal Dominant. One recessive case with mutation p.H222Y	Slow progressive contractures and muscle weakness involving elbows, Achilles tendons and post-cervical muscles, wasting of skeletal muscle and cardiomyopathy.
Dilated Cardiomyopathy (DCM)	Striated Muscle	Autosomal Dominant	Ventricular Dilatation, impaired systolic function and conduction system disease.
Limb Gridle Muscular Dystrophy (LGMD)	Striated Muscle	Autosomal dominant	Slow progressive pelvic girdle and shoulder muscle weakness. Later development of cardiac disturbance
Familial partial lipodystrophy-Dunnigan variety (FPLD)	Partial lipodystrophy	Autosomal Dominant	Subcutaneous fat loss, adipose tissue accumulation in face and neck, insulin resistance and diabetes.
Charcot-Marie-Tooth disorder type 2B1 (CMT)	Peripheral neuropathy	Autosomal Recessive	Motor and sensory neuropathies. Axonal degeneration. Muscle weakness and walking difficulties.
Limb Girdle Muscular Dystrophy (LGMD)	Striated	Autosomal Dominant	Slow progressive pelvic girdle and shoulder muscle weakness. Later development of cardiac disturbances.
Hutchinson-Gilford progeria syndrome (HGPS)	Progeria	De novo mutations. C to T change at codon 608 in exon 11 of *LMNA*, which activates a cryptic splice site, and generates a permanently farsenylated protein with 50 amino acids deleted at the C-terminus	Slow progressive pelvic girdle and shoulder muscle weakness. Later development of cardiac disturbances.

5.6 Discovery of MLIP

Muscle enriched A-type **L**amin **I**nteracting **P**rotein (**MLIP**) is a novel non-homologous, single copy gene found only in amniotes. Our laboratory discovered MLIP through a yeast two hybrid targeting the human heart and ventricular cDNA library. The assay used the N-terminal part of lamin A/C (10-230 amino acid) as bait due to the high number of mutations that span across these first 230 amino acids, which primarily result in dilated cardiomyopathy (Figure 4). It was found that MLIP is expressed in high levels in the heart, smooth, skeletal muscles while having low expression in the thymus, lungs and the liver (Figure 5). MLIP was found to interact directly with lamin A/C and co-localize in the nuclear envelope (Ahmady *et al*. 2011). Furthermore, another group have identified that MLIP possess an Islt-1 binding domain on exon 3 of *MLIP* (Huang *et al* 2012), which is a LIM/homeodomain transcription factor essential for differentiation of the second heart field cardiac progenitors. In addition, MLIP contains an AT-hook DNA binding domain on the C-terminus indicating it could play a potential role in transcriptional regulation (Huang *et al* 2012). Moreover, MLIP was found to have the ability to inhibit hypertrophy in cardiomyocytes via regulation at the transcriptional level; Over expression of MLIP resulted in no significant change to cardiomyocytes. However MLIP, significantly attenuated PE-induced hypertrophy and quantification of cardiomyocyte size confirmed that observation. At the level of gene expression, PE-induced expression of hypertrophic markers genes (ANP,BNP and ß-MHC) were inhibited by MLIP, suggesting that MLIP negatively regulates cardiomyocyte hypertrophy (Huang *et al* 2012). Finally, MLIP null mice exhibit normal cardiac

function despite myocardial Akt/mTOR pathways, Cardiac specific MLIP overexpression led to an inhibition of Akt/mTOR providing key evidence of a direct impact of MLIP on these key signaling pathways. Genome Wide Association showed genetic association between MLIP and early response to cardiac stress supporting MLIP's role in cardiac adaptation (Cattin, et al. 2015).

The human MLIP gene is located on chromosome 6p12.1 and is flanked by two genomic organizations, LRRC1 and TINAG, which are conserved in amniotes (mammals, reptiles, birds). The LRRC1 gene is conserved in bony vertebrates while the TINAG gene is conserved in *Drosophila* and *C. elegans*. (Ahmady *et al*. 2011), Indicating that MLIP is a single copy gene that is an innovation of placental mammals. Protein sequence alignment of full length MLIP in mouse, chicken and human revealed that MLIP contains at least five highly conserved domains. Domain 1 contains the lamin A/C interacting domain (amino acid 1-147) and putative sumoylation site. Domains 2 and 3 have an unknown function while domain 4 contains a putative nuclear localization sequence. Finally, domain 5 has an unknown function and contains a highly conserved putative tyrosine-phosphorylation site (amino acid 803-895) (Ahmady *et al*. 2011).

A yeast two-hybrid screen using MLIP as bait, in the search for MLIP interactors in the heart, identified LMNA, PKM2 and LMO7 as potential interactors (Figure 6a). LMO7 is a LIM/homeodomain transcription factor that is alternatively spliced and is expressed in most tissue. LMO7 functions as a transcriptional activator (Dedeic *et al* 2011). PKM2 is an iso-enzyme of the glycolytic enzyme

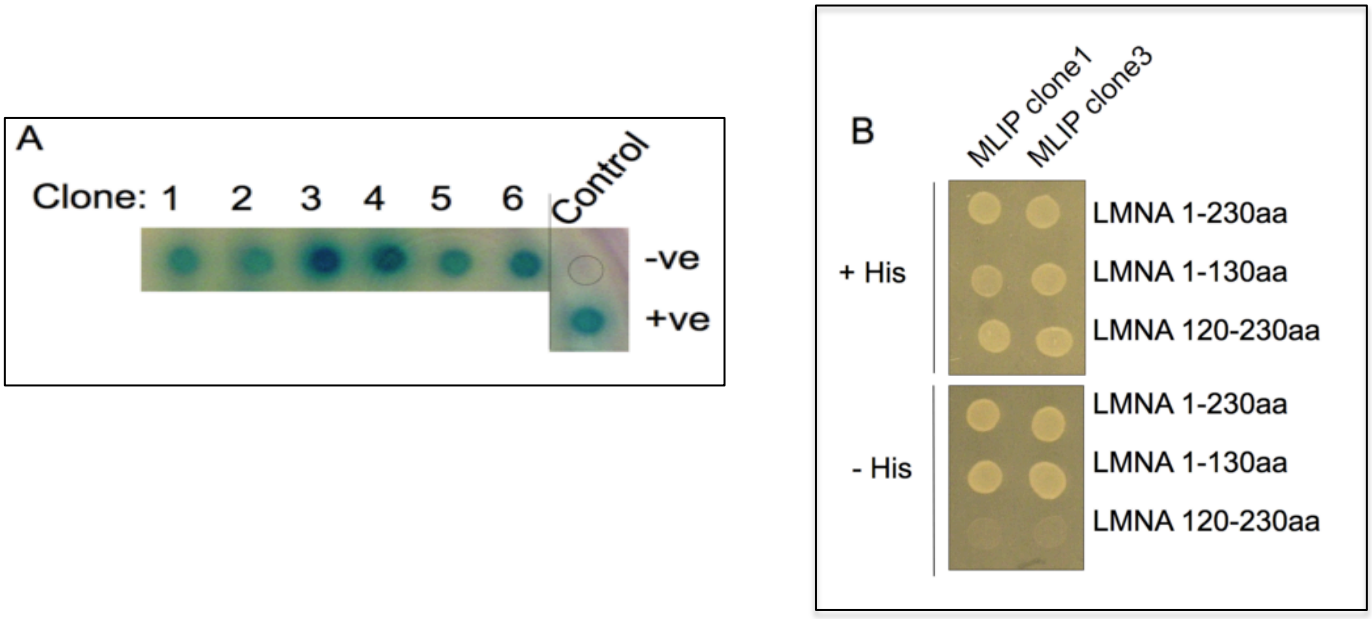

Figure 4: The interaction of Lamin A/C with MLIP, a Muscle Lamin Interacting Protein. **A)** A yeast-two hybrid interaction assay identified 6 independent MLIP clones from a human heart cDNA library (Clontech). **B)** Yeast-two hybrid assay of the LMNA1-230, LMNA1-130 and LMNA120-230 and MLIP clone 1 and MLIP clone 3 interactions. Twenty microliters of the culture was plated on His+ (left) and His- (right) plates at a cell density of 1x106/mL. (Ahmady et al JBC 2011)

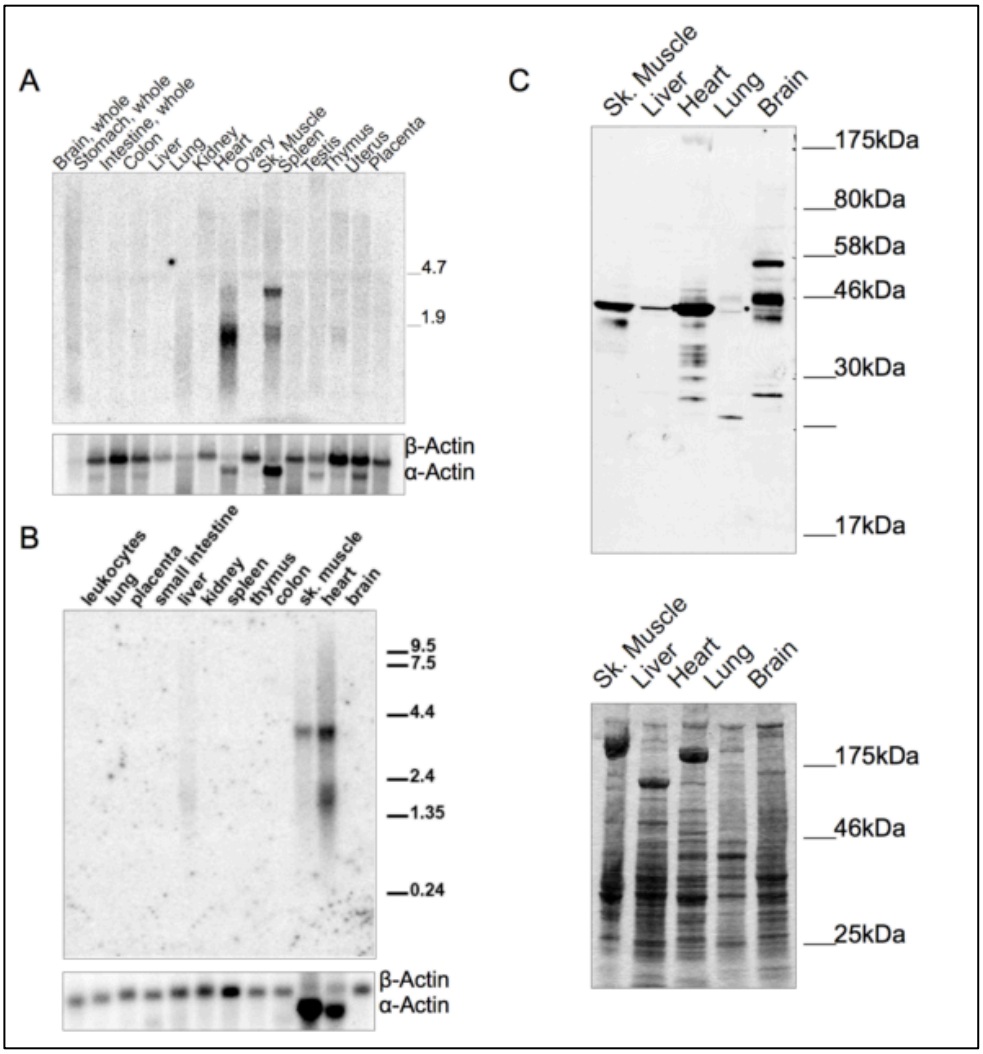

Figure 5: MLIP tissue expression profile. Expression of MLIP mRNA in A) mouse and B) human tissue by Northern analysis revealed two transcripts. 10ug of poly-A enriched RNA was loaded per lane. A human beta-actin cDNA fragment was used to probe the blots as an internal loading control. The beta- actin probe cross-hybridizes with alpha cardiac and alpha skeletal actin, that show up in the heart and skeletal muscle lanes. C) Endogenous tissue distribution of MLIP protein by Western analysis. 5#g of total soluble protein lysates from each tissue was loaded per lane as represented by coo-massie blue staining of total protein, lower panel (Ahmady et al JBC 2011).

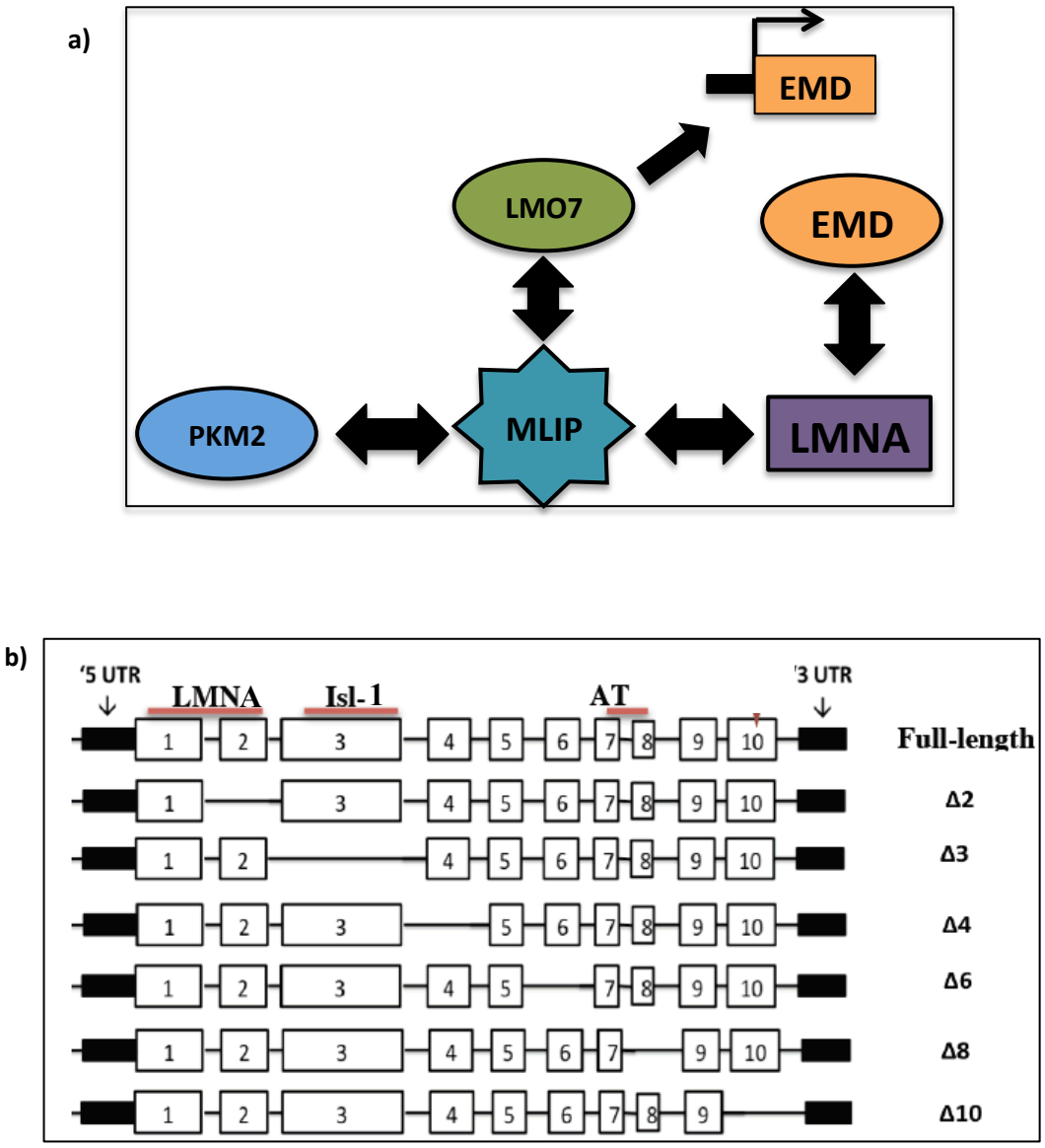

Figure 6: Human MLIP heart Interactors a) Schematic diagram of MLIP and its interactors that resulted from the yeast two hybrid in the search for MLIP heart interactors. b) Human MLIP isoforms, Schematic diagram demonstrating the different MLIP isoforms that have been chemically synthesized by IDT and sequence verified (Δ2, Δ3, Δ4, Δ6, Δ8, Δ10 and Full-length). MLIP isoforms showing the LMNA and Isl-1 binding sites are highlighted as well as putative AT-hook DNA binding domain.

pyruvate kinase, which is expressed in some differentiated tissues, such as lungs and fat tissue as well as cells with high rate of DNA synthesis, such as normal proliferating cells, embryonic cells and primarily tumor cells (Christofk et. al. 2008).

b) Rationale, Objective, Hypothesis and Aims:

Rationale:

The yeast two hybrid conducted using the first 230 amino acids of the Lamin A/C lead to the discovery of MLIP (Figure 4). The lamin binding domain was proven to be within the first 41 amino acids of MLIP protein, which spans across exon 1 and 2 of the MLIP gene (Figure 7) (Ahmady *et al*. 2011). Lamins are expressed in differentiated cells and Lamin A/C expression profile begins in the post-natal stages of heart development (Table 2). By means of immunoprecipitation, pre-natal hearts

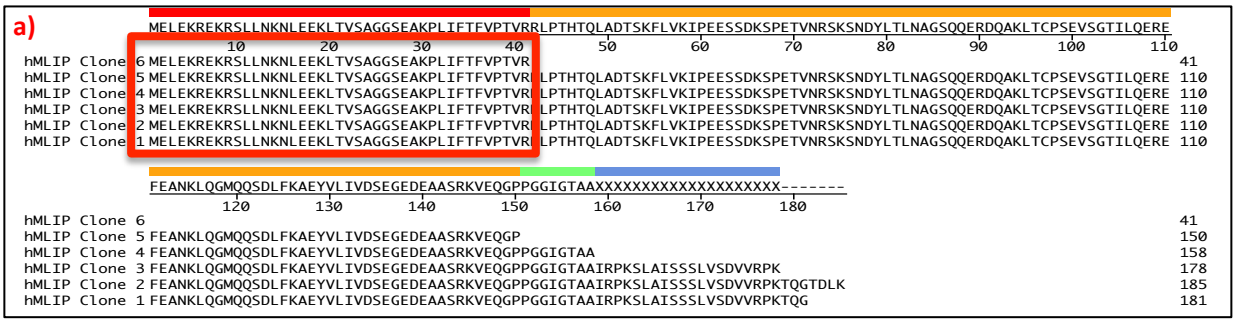

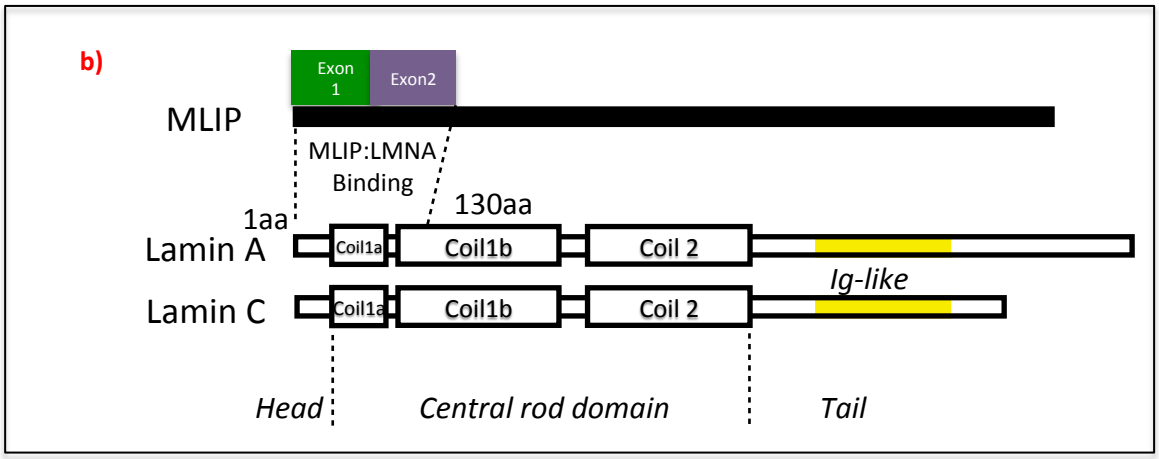

Figure 7: The Lamin A/C Binding Domain Spans across MLIP protein encoded by Exon 1 and 2 of the MLIP gene. **A)** Schematic diagram shows the 6 independent clones the resulted from the yeast two hybrid, where MLIP:Lamin A/C interaction was discovered all six clones were sequenced and aligned, where the overlapping occurs in the first 41 amino acids of the MLIP protein (exon 1 and 2). B) Displays MLIP:Lamin A/C binding domain.

Table 1. *Lamin A/C expression as judged by positive staining with mAB346*

	Embryonic day									Postnatal day				
	9	10	11	12	13	14	15	16	17	1	5	10	15	Adult
Decidua	+++	+++												
Trophoblast	+++	+++												
EMBRYO PROPER														
Mesenchyme/ Connective tissue*	–	–	d	s	s	m	+++	+++	+++	+++	+++	+++	+++	+++
Muscle†														
Appendages†	–	–	d	m	+++	+++	+++	+++	+++					
Trunk†	–	–	–	m	+++	+++	+++	+++	+++					
Eye muscle†	–	–	–	m	+++	+++	+++	+++	+++					
Skeletal muscle										+++	+++	+++	+++	+++
Heart	–	–	–	–	–	–	–	–	–	–	m	++	+++	+++
Vessels‡														
Umbilical	–	–	–	+	+	+	+	++	++					
Aorta	–	–	–	(+)	+	+	+	++	++	++	++	++	++	++
Epithelia														
Epidermis	–	–	–	–	–	d	+	+++	+++	+++	+++	+++	+++	+++
Tongue									++					++
Intestine	–	–	–	–	–	–	–	–	–	–	–	–	–	+§
Liver	–	–	–	–	–	–	–	–	–	–	m	+++	++	+++
Lung	–	–	–	–	–	–	–	–	–	m	+++	+++	+++	+++
Kidney tubule	–	–	–	–	–	–	–	–	–	–	m	++	+++	
Nasopharynx	–	–	–	–	–	–	–	–	–	–	m	+	++	
Brain	–	–	–	–	–	–	–	–	–	–	m	m	+++	+++
Spleen													m	m
Thymus													m	m
Bone marrow														m

<u>Table 2</u>: Lamin A/C embryonic stem cell differentiation marker, this table displays the level of expression of lamin A/C in tissue, both embryonic and post-natal stages of development. Permission granted by CC-BY licence. Röber RA, Weber K, Osborn M. Differential timing of nuclear lamin A/C expression in the various organs of the mouse embryo and the young animal: a developmental study. Development. 1989 Feb.

were used to confirm the MLIP-Lamin interaction (Ahmady *et al*. 2011). MLIP is ubiquitously expressed and heavily spliced in different tissues (Figure 5), with at least 7 known variants discovered (Δ2, Δ3, Δ4, Δ6, Δ8, Δ10 and Full length) (Figure 6). MLIP's expression differs in tissue and MLIP is subjected to extensive tissue-dependent alternative splicing. MLIP's biological function remains largely unknown but it may be of high relevance for muscle function due to its abundant expression in the heart, skeletal and smooth muscles.

Objective:

The main **objective** of this study was to map the exact location of MLIP:Lamin A/C binding domain and the identification of MLIP isoform specific binding partners in different tissues. To achieve this, we addressed the question: **How does tissue specific alternative splicing of MLIP modulate its affect in different tissue?**

Hypothesis:

We **hypothesized** that the MLIP:Lamin A/C binding domain is protein specific interaction that is encoded by exon 1.

We also **hypothesized** that the phenotypic observations in laminopathies may be in part due to the differential MLIP isoform expression pattern in tissue, whereas MLIP isoforms have different binding partners in different tissues resulting in variable functions.

Aims:

1) **To define MLIP-Lamin A/C Binding Domain; mapping the binding domain and proof of concept of the unique site this interaction possesses.**

   Methods Employed: Recombinant protein expression, Glutathione S-Transferase purification, Co-Immunopreciptation and Western Blot.

2) **Characterization of MLIP expression profile in tissue and it's binding partners.**

   Methods Employed: Western Blot analysis.

3) **Characterization of MLIP expression profile in perinatal heart and the splice variants expressed during post-natal development.**

   Methods Employed: RT-PCR (Reverse Transcriptase-PCR) and Western Blot Analysis.

Chapter 2:
Materials and Methods

6.1 Generating GST-hLamin

LMNA cDNA used in the yeast two hybrid which contained the first 230 amino acid of the *LMNA* gene was sub-cloned into a GST-tag fusion vector pGEX-2t (GE healthcare Life Sciences) (Figure 8) and transformed into the bacterial strain BL21 DE3. The bacterial cells were up-scaled and during the exponential growth phase, isopropyl-1thio-D-galactopyranoside (IPTG) was added for a final concentration of 1mM and the culture was incubated for 2 hours at 37°C with shaking (250 rpm), followed by a 10 minute 4400g (5000 rpm) centrifugation at 4°C. The pellet was stored at -80°C.

6.2 Bacterial Cell Lysis

Bacterial cells were thawed then lysed in (20mM Tris-HCl, 500mM NaCl, 10% Glycerol; pH 7.9), 5mM $MgCl_2$, 0.2mg/mL Lysozyme (Sigma), 10 units of RQ1 RNase-Free DNase and 1x Protease Inhibitor cocktail (Roche, 1 tablet/10.0 mL). The cell lysate was vortexed until every component has dissolved at 4°C, followed by 3 freeze thaw + sonication (40 sec/cycle) cycles. The cell lysate was then centrifuged at 27,000g (15,000 rpm in JA-20 rotor) for 20 minutes at 4°C and the pellet was discarded.

6.3 Purification of rGST-hLamin

The GST-tag recombinant Lamin was purified using Glutathione Sepharose™ 4B(GE Health Life Sciences). 1mL of the beads were washed with Binding buffer (PBS, pH 7.3 (140mM NaCl, 2.7mM KCl, 10mM NA_2PO_4, pH7.31)). The sample containing the

a)

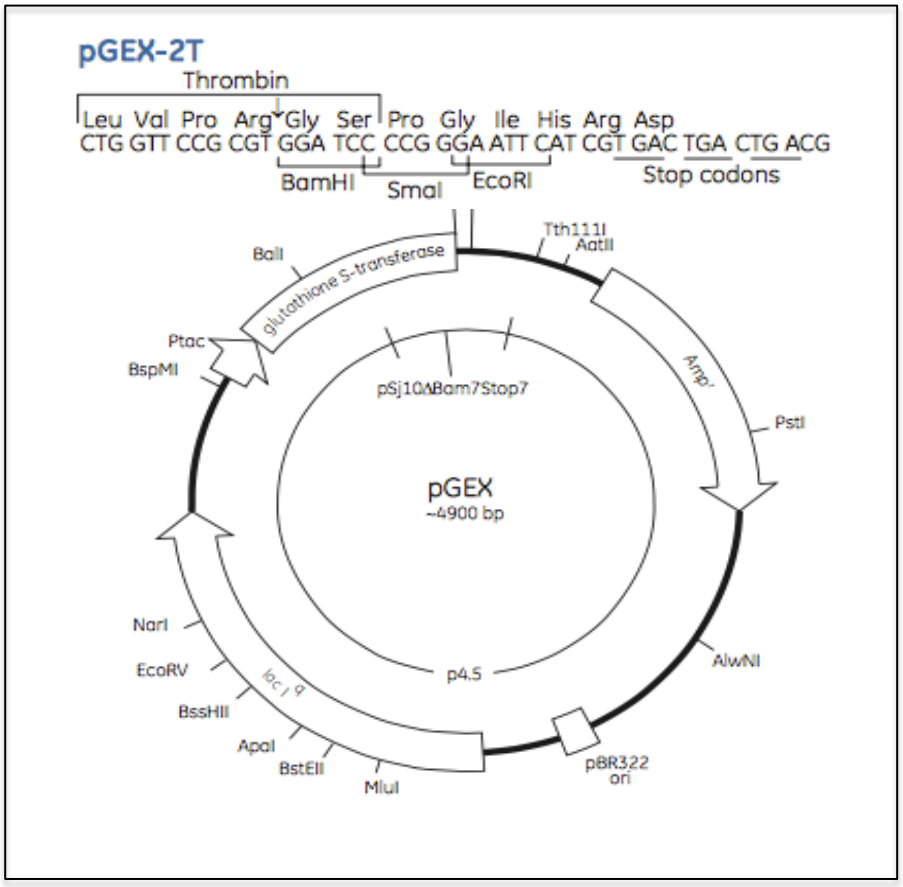

b)

Figure 8: Schematic diagram of the pGex-2t: GST-hLamin A/C plasmid and Protein. a) GST-LMNA in pGEX-2t contains the lamin A/C construct that was originally used in the yeast two hybrid (exons 1, 2, 3 and part of exon 4 of the LMNA gene). b) Schematic diagram of the GST-Lamin A/C protein which consists of a GST-tag (on its N-terminus) and a linker connecting it to Lamin A/C.

GST-Lamin was applied to the Glutathione Sepharose beads was gently shaking at room temperature for 30 minutes and the sample was loaded onto empty chromatography column (INCSTAR) the flow rate was gravitational. The column was washed with Binding buffer. Elution was performed using elution buffer (50mM Tris-HCl, 10mM reduced glutathione, pH 8.0) was eluted out by the gravitational force and four 1mL fractions were taken. The four fractions collected were loaded onto a PD-10 desalting column (GE Healthcare) and desalted with PBS and stored in 4°C.

6.4 Immunoblotting for MLIP in mouse tissue

Male adult mouse Brain, Heart, Skeletal Muscle, Spleen, Liver, Pancreas and Thymus as well as post-natal hearts (Day 0.5, 1, 3, 5, 7, 10 and adult) were harvested from 129SV mice. The Skeletal muscle included all muscles found in the leg. Tissues were lysed in 50mM Tris-HCl (pH8.0), 200mM NaCl, 20mM NaF, 20mM β-glycerolphosphate, 0.5% NP-40, 0.1mM NA3VO4, 1x Protease Inhibitor cocktail (Roche, 1 tablet/10mL), and 1x Phosphotase inhibitor tablet (Roche 1 tablet/10mL) using a glass homogenizer. Lysates were incubated on ice for 20 minutes and then cleared by centrifugation at 10,000xg for 10 minutes at 4°C. Supernatants were collected and protein concentrations were determined using Bio-Rad protein assay dye reagent concentrate kit (Biorad) and values read using the Thermo Electron Corporation Helios UV-Visible Spectrophotometer.

Twenty micrograms of protein was resolved on a 12% 1.00mm thick SDS-Tris Glycine polyacrylamide gel at 200V (Biorad Gel Apparatus) and transferred to PVDF

membranes (Millipore) for 1 hour at 100V. Transfer buffer was composed of 190mM glycine, 25mM tris- base and 20% cold methanol. Following protein transfer, membranes were blocked in 5% fat free milk (Carnation Instant skin milk powder) dissolved in Tris-base-Tween-20 (TBS (500mMtris,1.5M NaCl), 0.05% Tween-20) for 1 hour. Membranes were then incubated in MLIPc, MLIP 1a, MLIP 1b polyclonal antibody (1:5000, 1;1000, 1:5000, respectively) in 5% fat free milk overnight with gentle shaking at 4°C. Polyclonal Antibodies to MLIPc and MLIP 1b were raised in rabbit against **MLIP1a**: MEFGKHEPGSSLKRNKNLC-amide **MLIP-1b**: MTSCILAGSLETTPK-Ahx-[K-hydrazino]-amide **MLIP-C**: Ac-LRKDEEVYEPNPFSKYLC-amide) (Table 3). Membranes were then incubated with Anti-rabbit IgG, HRP-linked Antibody (Cell Signaling) for 1 hour at room temperature with gentle shaking. Immunoblot signals were detected using a SuperSignal West femto Chemiluminescent Kit (Thermo Scientific) and was developed using Molecular Imager® Chemi Doc™ XRS+ Imaging System (Bio Rad).

Table 3: Displays the MLIP polyclonal antibodies and the amino acid sequence it is targeted against along with the source of the antibody.

Antibody Name	**Epitope Directed against**	**Source**	**Epitope Exonic location**
MLIP-1a	MEFGKHEPGSSLKRNKNLC	Rabbit	1a
MLIP-1b	MTSCILAGSLETTPK	Goat	1b
MLIPc	LRKDEEVYEPNPFSKYLC	Rabbit	10

6.5 Generating MLIP's Isoforms in TnT (Transcription and Translation) Systems

In vitro transcription and translation reactions were performed with the TnT-coupled wheat germ extract system on Vector pIDTBlue:Myc-hMLIP delta 2, 3, 4, 6, 8, 10 and Full Length MLIP (Figure 11). A 50ul reaction using Wheat Germ Extract Systems consists of 25ul TnT Wheat Germ Extract, 2ul TnT Reaction Buffer, 1ul TnT polymerase, Amino Acid minus methionine and Amino acid minus cysteine, 1ul RNasOUT Ribonuclease Inhibitor and the DNA Template. The reaction was incubated at 30°C for 1 hour. Samples were prepared for western blot analysis as described below.

6.6 SDS-PAGE, Coomassie Staining and Immunoblotting of rGST-hLMNA

Proteins were resolved on a 12% (w/v) 1.00mm thick SDS-TrisGlycine polyacrylamide gel at 200V (Biorad Gel Apparatus). The gel was either subjected to Coomassie staining (0.2% (w/v) Coomassie Blue, 7.5% Acetic acid (v/v), 50% Ethanol (v/v)) for 1 hour at room temperature followed by an overnight destaining (50% Methanol (v/v), 10% Acetic acid (v/v)), or proteins were transferred to a PVDF membranes, (Millipore) for 1 hour at 100V. Transfer buffer was composed of 190mM glycine, 25mM tris- base and 20% cold methanol (v/v). Following protein transfer, membranes were blocked in 5% fat free milk (Carnation Instant skin milk powder) dissolved in Tris-base-Tween-20 (TBS (500mM Tris,1.5M NaCl), 0.05% Tween-20 (v/v)) for 1 hour. Membranes were then incubated in GST polyclonal antibody (Cell Signaling) (1:1000) in 5% fat free milk (w/v) overnight with gentle

a)

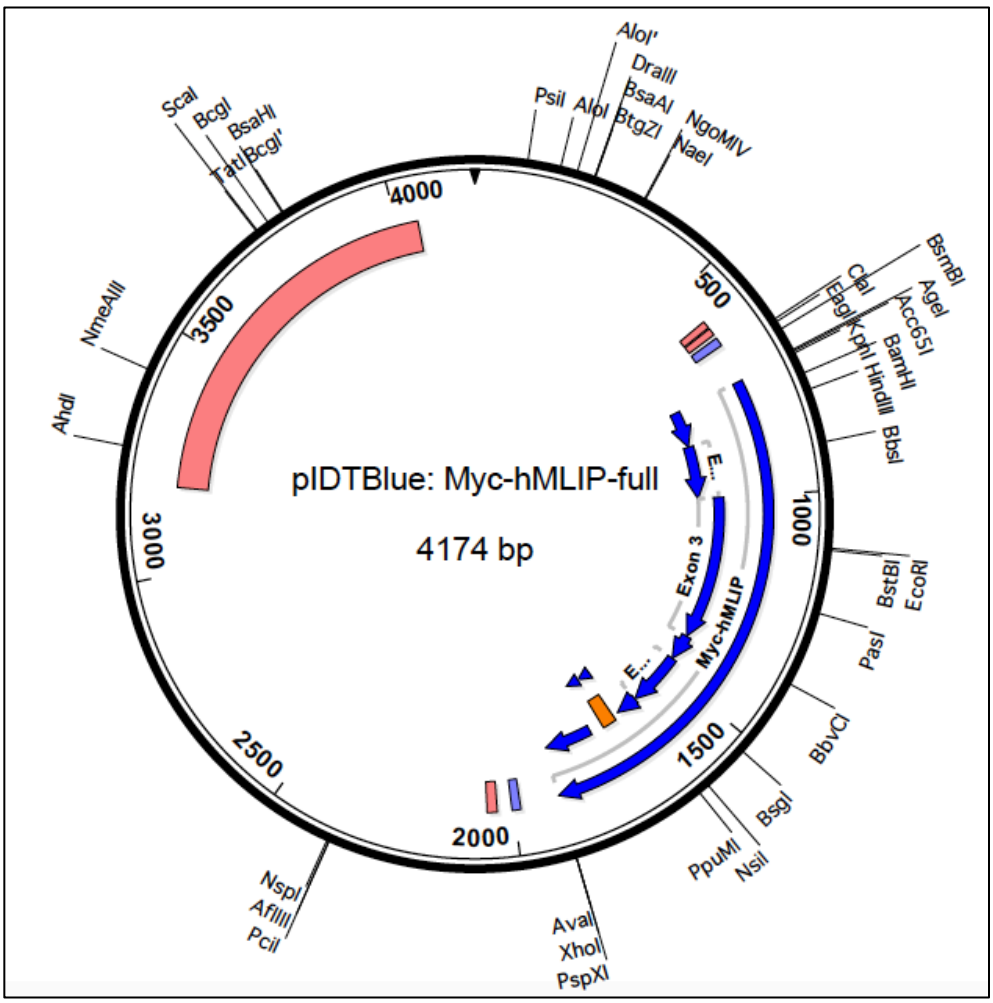

b)

Figure 11: Schematic diagram of the pIDTBlue: Myc-hMLIP plasmid and Protein. a) pIDTblue is a chemically synthesized plasmid of human MLIP and its isoforms (Δ2, Δ3, Δ4, Δ6, Δ8, Δ10) by IDT and sequence verified the plasmid contains a T7 promoter and the MLIP gene is in the T7 orientation (E= exon). b) Schematic diagram of the MLIP protein which consists of a Myc-tag on its N-terminus.

shaking at 4°C. Membranes were then incubated with Anti-rabbit IgG, HRP-linked Antibody (Cell Signaling) for 1 hour at room temperature with gentle shaking. Immunoblot signals were detected using a SuperSignal West femto Chemiluminescent Kit (Thermo Scientific) and was developed using Molecular Imager® Chemi Doc™ XRS+ Imaging System (Bio Rad).

6.7 Immunoprecipitation: MLIP:Lamin Pull down

MLIP Delta 2, Delta 3, MLIP Full length and MLIP 1b were generated by TnT Systems (In-vitro Transcription and Translation) resulting in 50ul of lysate. 10ul of the purified rGST-hLamin were added onto the lysate. 10ul were taken out as input, following the wash of the beads with 500ul of Binding buffer and 30ul Glutathione Sepharose beads (GE Healthcare) were added to the lysate mixture (hMLIP+rGST-hLamin) and incubated at room temperature for 1 hour on the rocker, The lysate + the beads are transferred into a spin column and centrifuged at 3000g (1100 rpm) the beads are then washed with 500ul of PBS. Then 40ul of Elution buffer is then added (50mM Tris-HCl, 10mM reduced glutathione, pH 8.0) to the beads and is incubated for 1-2 minutes before the elution buffer is spun down. The collected Elute is then prepared for western blot analysis.

6.8 Identification of Mouse MLIP Splice Variants in the Heart and Brain

Total RNA was extracted using Trizol (Invitrogen) as manufacturer's instructions (performed by Cassie Roeske). 1.0ug of RNA was reversed transcribed using Transcriptor Reverse Transcriptase (Roche). cDNA was amplified with

primers (IDT) designed to the 5' End Exon 1b (5' – ATG ACC TCC TGC ATC TTA GCG GGG A– 3') and Exon 1a (5' –ATG GAA TTT GGA AAG CAT GAA CCA GGA AGC– 3') and to the 3' End of 67 reverse (5'–GGG TTG GGC TCA TAA ACT TC– 3') and PCR anchor (5'–GAC CAC GCG TAT CGA TGT CGA C– 3'). cDNA Amplification was carried out as follows: 98°C for 30 seconds, followed by 35 cycles in 3 steps: 98°C for 5 seconds, 60°C for 15 seconds, and 72°C for 3 minutes and 72°C for 2 minutes using Q5® High-Fidelity (NEB). PCR products were confirmed by analysis on a 1% agarose gel stained with ethidium bromide. Heart and Brain lysates were lysed and compared mRNA to protein expression and probed MLIPc and MLIP 1b polyclonal antibodies.

6.9 Cloning Strategy to Identify Human MLIP 1b Splice Variants

MegaMan Human Transcriptome Library is a collection of cDNA created using mRNA from 66 diverse sources, including 32 from human tissues and 34 from human cancer cell lines. cDNA was amplified with primers (IDT) designed to the putative 5' and 3' ends of MLIP 1b. The primer sequence for forward and reverse (MLIP 1b fwd 5'–ATG ACC TCC TGC ATC TTA GC–3'; MLIP 1b rev 5'–TCA CTG TTC AGA AAA GAG GTC GC–3'). Gene Amplification was carried out as follows: 95°C for 30 seconds, followed by 30 cycles in 3 steps: 95°C for 10 seconds, 57°C 15 seconds, 68°C for 4 minutes and 72°C for 5 minutes using DNA Taq Polymerase (NEB). PCR products were confirmed by analysis on a 1% agarose gel stained with ethidium bromide. PCR products were inserted into the pGEM-T vector System (Promega A3600) according to manufacturers instructions (Figure 13). Plasmids were transformed using NEB 10-β (NEB) Chemically Competent *E. coli* according to

manufacturer's instructions. Plasmids were sequenced using primers to T7 (TAATACGACTCACTATAGGG) and SP6 (ATTTAGGTGACACTATAG) promoters (Figure 14).

Isolation of the hMLIP-1b splice variants was performed by Esther Mak-Washburn.

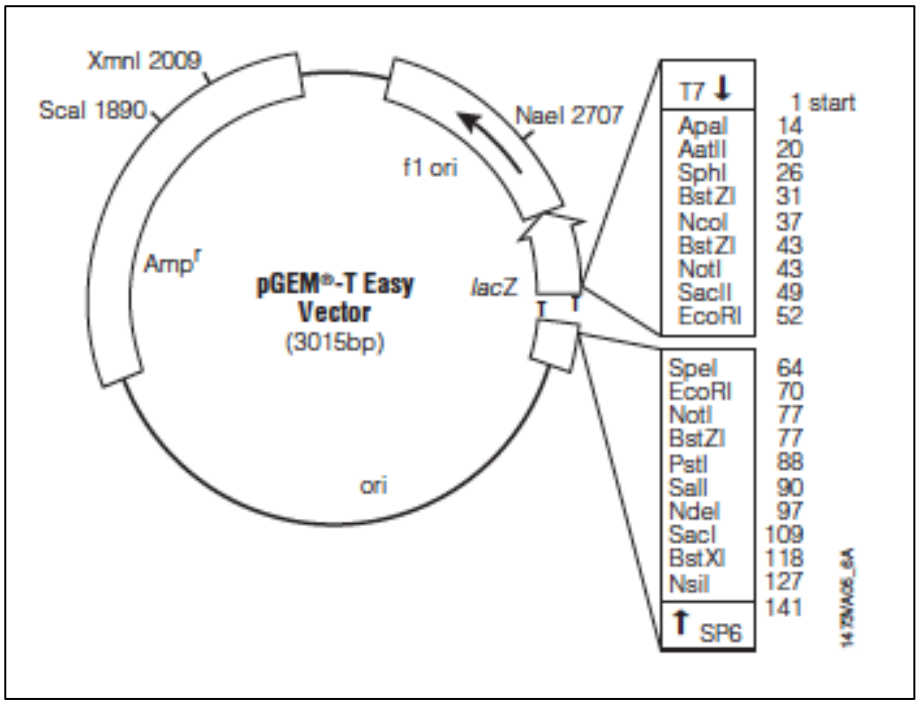

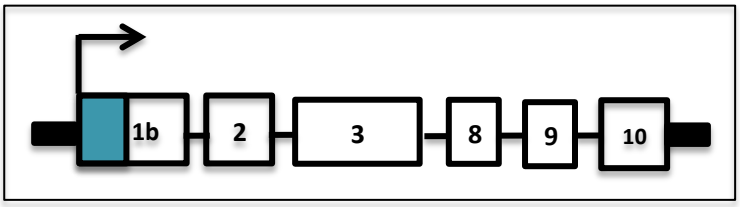

<u>Figure 13</u>: Schematic diagram of the pGEM-T: hMLIP 1b Clone #1 plasmid and Protein. MLIP 1b in pGEM-T contains exons 1b, 2, 3 , 8, 9 and exon 10 of the MLIP gene and its expected size is 30 kDa.

hMLIP -1b (DNA Sequence)

ATGACCTCGTGCATCTTATCAGGGAGCATTCAGACCACACCCCAGGTCTCTGCTGGTGGTTCTGAAGCCAAACCTCTGATCTTCACATT
TGTCCCCACTGTCAGAAGACTACCAACCCATACTCAGTTGGCTGACACCTCTAAATTCCTTGTTAAAATTCCAGAAGAATCAAGTGATA
AGAGTCCAGAAACTGTAAATAGGTCTAAATCCAATGACTACTTGACCTTGAATGCTGGGAGCCAACAAGAGAGAGACCAAGCGAAA
TTGACTTGTCCTTCAGAGGTCAGTGGAACGATTTTACAAGAAAGGGAATTCGAAGCAAACAAACTTCAAGGGATGCAGCAAAGTGA
CCTCTTCAAAGCTGAATATGTCCTTATTGTGGACTCCGAAGGGGAAGATGAGGCTGCAAGCAGAAAAGTTGAACAAGGCCCCCCAGG
GGGGATTGGCACCGCAGCTGTCCGGCCCAAGTCTCTAGCTATCTCGTCCAGTCTGGTCTCTGATGTAGTGCGTCCCAAAACACAGGGG
ACTGATCTCAAGACCTCATCACATCCTGAAATGCTTCATGGGATGGCCCCTCAGCAAAAGCATGGGCAGACTCCTACAACTCTTCCAA
GAGCAGCTGGTCGAGAAACCAAATATGCAAATCTCTCCTCACCATCTTCTACAGTATCTGAGAGTCAGCTGACTAAGCCTGGAGTAAT
TCGCCCAGTACCTGTAAAATCCAGAATATTACTGAAAAAAGAGGAGGAAGTCTATGAACCCAACCCTTTCAGTAAATACTTGGAAGA
TAACAGCGACCTCTTTTCTGAACAGTGA

hMLIP -1b (Amino Acid Sequence)

MTSCILSGSIQTTPQVSAGGSEAKPLIFTFVPTVRRLPTHTQLADTSKFLVKIPEESSDKSPETVNRSKSNDYLTLNAGSQQERDQAKLTCPSE
VSGTILQEREFEANKLQGMQQSDLFKAEYVLIVDSEGEDEAASRKVEQGPPGGIGTAAVRPKSLAISSSLVSDVVRPKTQGTDLKTSSHPE
MLHGMAPQQKHGQTPTTLPRAAGRETKYANLSSPSSTVSESQLTKPGVIRPVPVKSRILLKKEEEVYEPNPFSKYLEDNSDLFSEQ.

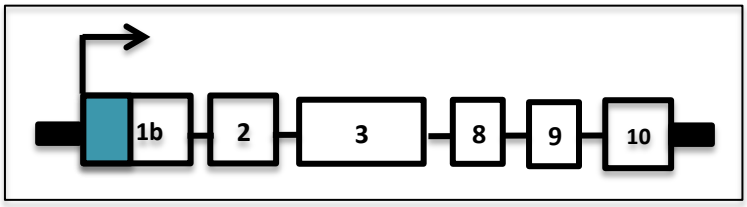

<u>Figure 14</u>: hMLIP-1b Clone #1: hMLIP -1b DNA sequence and amino acid sequence, Which contains exon 1b, 2, 3, 8, 9 and exon 10.

Chapter 3: Results

7.1 Synthesis and purification of rGST-hLamin

To identify the exon specificity of the MLIP:Lamin A/C binding domain, we first synthesized and purified rGST-hLamin using a bacterial cell culture system. The plasmid containing the GST-hLamin A/C (Figure 8) was transformed into BL21 bacterial high expression protein cells, which were harvested and lysed to extract and purify GST-Lamin via Glutathione sepharose beads. Efficiency of the transformation was assessed using SDS-gel stained with coo-massie Brilliant blue which showed the presence of the recombinant protein 50kDa (Figure 9, left). Further purification using column chromatography and western blot using an anti-GST antibody confirmed the present of the rGST-hLamin (Figure 9, right).

7.2 Generation of hMLIP splice variants

In order to synthesize the different hMLIP isoforms, we performed *in-vitro* transcription and translation (TnT) reactions on pIDTBlue:Myc-hMLIP delta 2, 3, 4, 6, 8, 10 and full length MLIP (Figure 6). The samples were prepared for western blot analysis and probed with MLIPc antibody, which targets the C-terminus epitope within exon 10 of MLIP. We were able to both confirm the successful production of the different hMLIP isoforms (Figure 10 A) as well as confirm the specificity of the MLIPc antibody since no band was detected in the delta 10 isoform lane (Δ2= 37kDa, Δ3=29kDa, Δ4= 39kDa, Δ6=42kDa, Δ8= 41kDa and Δ10=38kDa) (Figure 10 A). We also noted the presence of a second smaller band when probing with MLIPc

antibody, which was present in all isoforms except delta 3 (Δ2=29kDa, Δ4=25kDa, Δ6=28kDa, Δ8=27kDa and FL=29kDa) (Figure 10 A, and Table 4), and is a result of a

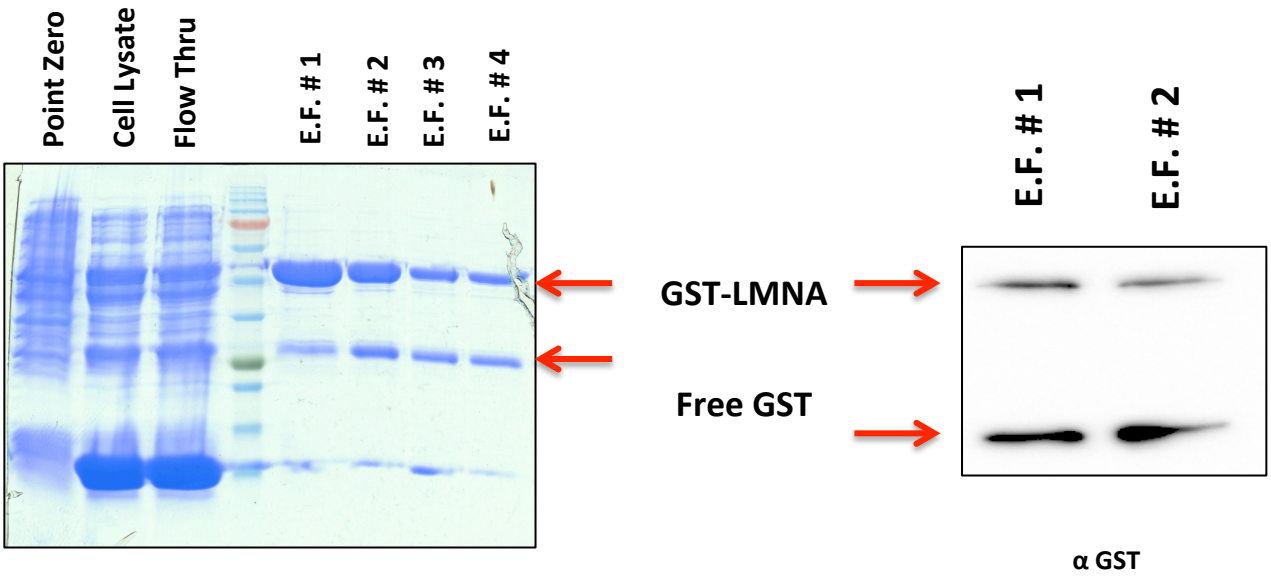

Figure 9: Recombinant GST-Lamin A/C Purification: pGEX-2t was transformed into BL21 high expression bacterial cells, the cells were grown and induced for 2 hours with1mM IPTG and cells samples were taken before induction and after induction as controls along with elution fractions (E.F.). Samples were detected via SDS gel stained with coo-massie brilliant blue and western blot via anti-GST.

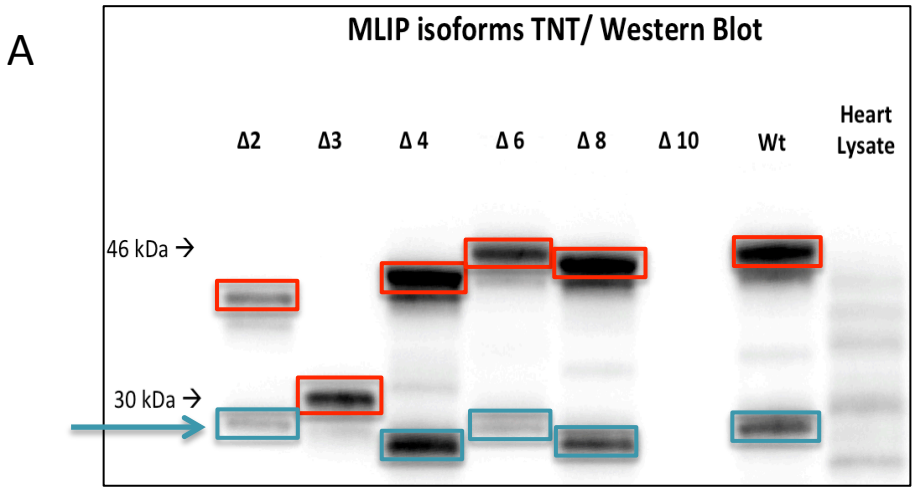

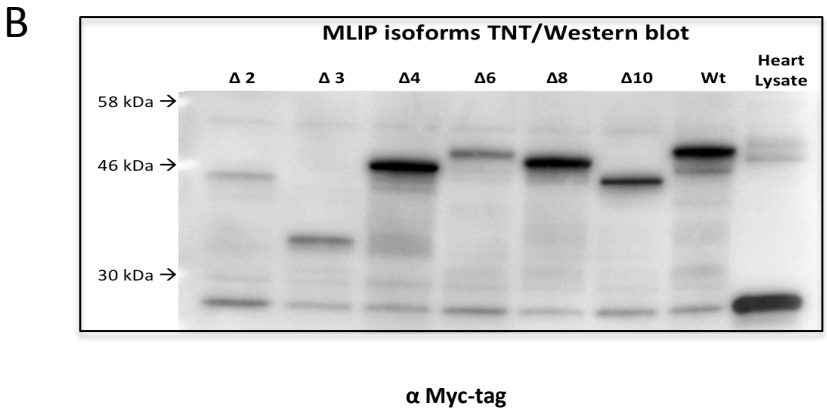

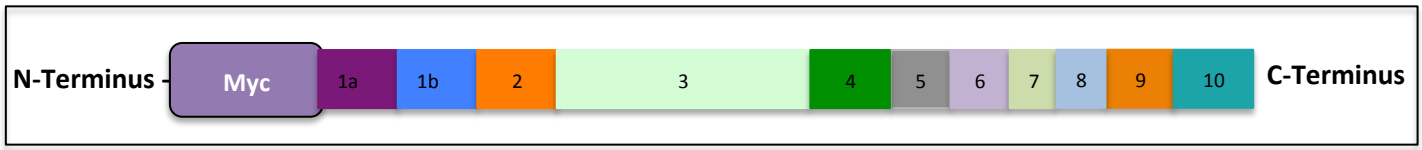

<u>Figure 10</u>: Generation of human MLIP isoforms Expression in TnT (Transcription Translation) Systems: Human MLIP isoforms construct used were chemically synthesized by IDT and sequence verified were in-vitro transcribed and translated in wheat germ cells for 2 hours, expressed protein was detected by SDS PAGE and probed with Anti-MLIPc (1:5000) and Anti-Myc (1:3000). The highlighted red box are the MLIP splice variants and delta 10 is an internal control because MLIPc antibody is directed against an epitope encoded within exon 10, and the presence of a secondary band found in all variant except delta 3 which are highlighted in blue boxes. When probing anti-myc the secondary band disappears suggesting an alternative start site found in exon 3.

Table 4: Displays the experimentally determined molecular sizes of in vitro transcribed-translated MLIP isoforms, probed with MLIPc antibody and Myc-epitope tag antibody.

MLIP Isoforms	**MLIPc Antibody** Size of protein kDa	**Myc- Antibody** Size of Protein kDa
MLIP Full length	44 kDa, 29 kDa	44 kDa
Δ2	37 kDa, 29 kDa	37 kDa
Δ3	29 kDa	29 kDa
Δ4	39 kDa, 25kDa	39 kDa
Δ6	42 kDa, 28kDa	42 kDa
Δ8	41 kDa, 27 kDa	41 kDa
Δ10	_____	38 kDa

ribosomal cleavage site or an alternative start site. To further investigate the identity of the additional band, we probed using a Myc-Tag antibody targeting the Myc epitope on the N-terminus of the synthesized isoforms (Figure 11). When probing for Myc, we were able to identify a single band per isoform (Figure 10 B), which lead us to believe the presence of an alternative start site present in exon 3.

In addition, we observed the presence a band that wasn't accounted for in the brain 58 kDa (Figure 5C), which led us to believe that there are extra exons or an alternative promoter we preformed a 5' and 3' RACE to amplify the MLIP gene the results revealed the presence of an alternative promoter in exon 1, which we annotate as 1b (Data not shown). To confirm the presence of an alternative promoter in exon 1, we used a MegaMan Human Transcriptome Library to amplify cDNA using primers targeting the putative MLIP 1b promoter and 9 and 10 MLIP exons. We obtained several different size PCR products (Figure 12 A), which were sub-cloned into the pGEM-T vector system. Plasmids were sequenced using primers to T7 and SP6 promoters, and the orientation of the insert was determined (Figure 12 B). We chose a single MLIP-1b clone, because that clone was largest in size, contained exon 1b, 2, 3, 8, 9 and exon 10 which we can detect with MLIPc antibody (Figure 13/14) to further perform TnT and IP experiments.

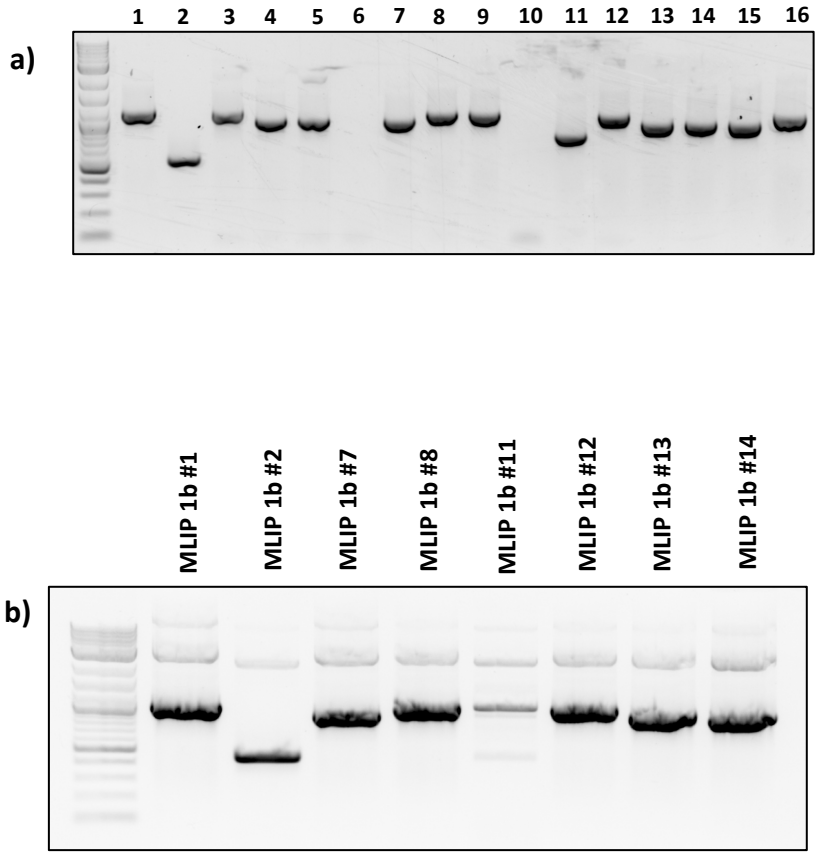

Figure 12: Sub-Cloning Human MLIP 1b Splice Variants: a) Human cDNA library (Megaman) was used to identify MLIP 1b splice variants that are encoded by exon 1. cDNA was amplified with primers designed to the 5' end exon 1b and amplifying the 3' end exon and the resulting variants were sub-cloned into pGEM-T vectors. b) PCR products for pGEM-T:hMLIP-1b and was amplified using SP6 primers to determine the orientation, which shows that the pGEM-ThMLIP-1b is in T7 orientation.

7.3 Assessment of MLIP:Lamin A/C Immunoprecipitation

We know from previous results that Lamin A/C binds to the first 41 amino acid of MLIP (Ahmady al. et 2011), which is encoded by the first two exons. Thus, to determine the exact location in MLIP that Lamin A/C binds to, we used the full length MLIP (FL MLIP), two MLIP isoforms (MLIP Δ2 and Δ3) as well as the MLIP-1b variant (MLIP 1b), which contains exons 1b, 2, 3, 8, 9 and 10 (Figure 14). We mixed the different MLIP isoforms with the purified rGST-hLamin, then pulled down with glutathione sepharose beads and probed the input and IP with MLIPc and GST antibodies.

When probing with MLIPc, we were able to detect all the MLIP isoforms in the input. On the other hand, after IP with Lamin, we were only able to detect the isoforms that contained the 1a exon (MLIP FL, Δ2 and Δ3) but not the 1b (Figure 15). We also probed with GST antibody showing the presences of GST-Lamin in the pull down. This suggests that MLIP Lamin binding domain is specific to MLIP exon 1a (Figure 15). We confirmed these results by repeating the experiment with an additional control using the FL MLIP and confirmed that the beads cannot pull-down MLIP without the presence of Lamin (Figure 22).

7.4 Endogenous Tissue Distribution of mMLIP Profile

To determine the tissue distribution of mouse MLIP (mMLIP), various tissues were isolated from male 129SV mice. Brain, heart, skeletal muscle, spleen, liver, pancreas as well as thymus were harvested and probed for MLIP. We also isolated and probed for MLIP in post-natal hearts since MLIP's discovery was through its

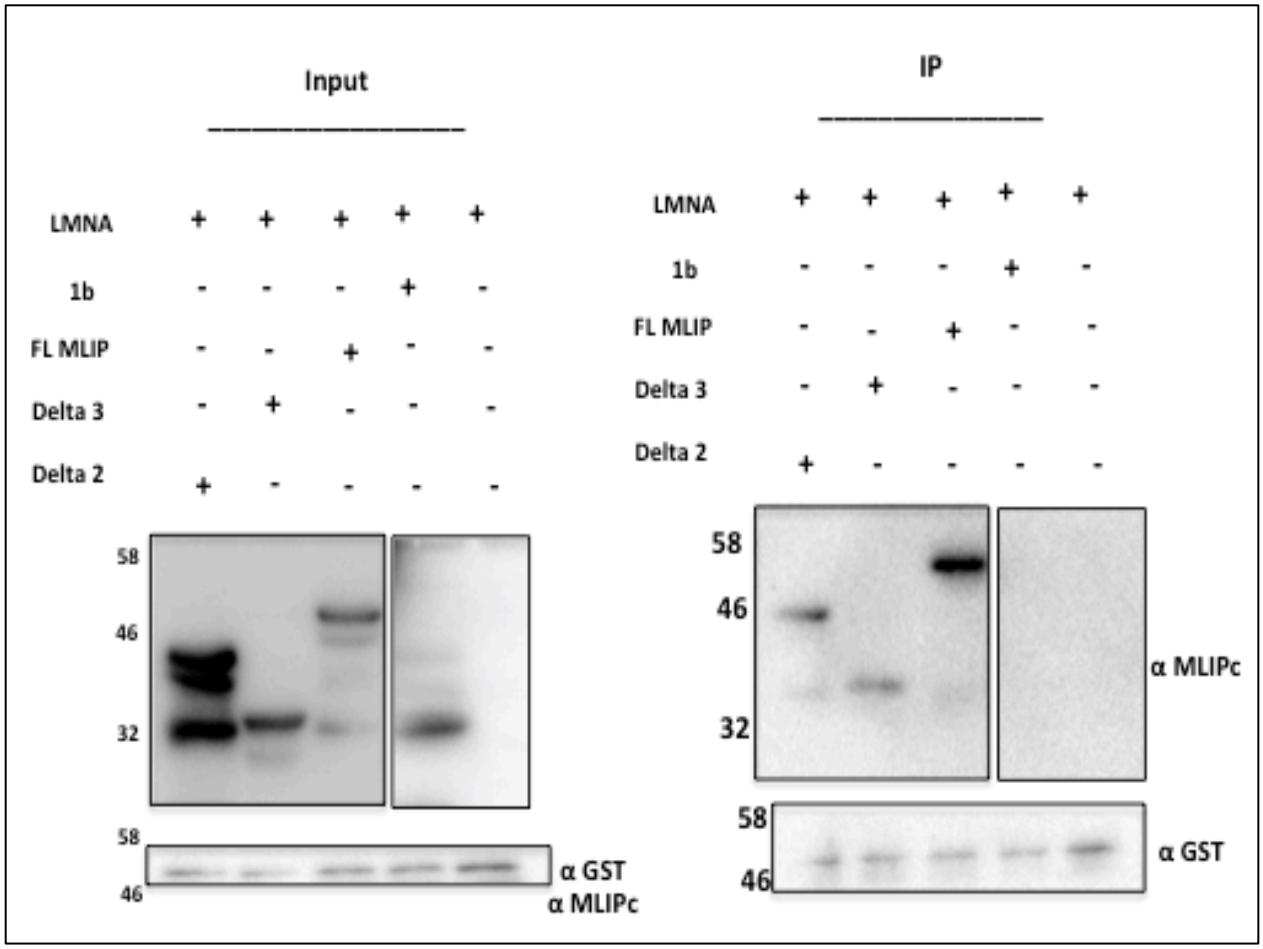

<u>Figure 15</u>: Purified recombinant GST-Lamin A/C binds directly with MLIP Specifically to the protein encoded by exon 1a in an in-vitro co-immunoprecipitation assay. A) Purified recombinant GST-Lamin A/C and TnT (Transcription Translation Systems) expressed MLIP isoforms were separately mixed together to form complexes precipitated through the Glutathione sepharose beads. Western analysis was performed using Anti-GST to determine the presence of lamin A/C in the pull down (1:1000) and Anti-MLIPc (1:5000) polyclonal antibodies to detect MLIP isoforms. B) The co-immunoprecipitation was performed as previously mentioned with an extra control.

interaction with Lamin and lamin is highly expressed at that stage of heart development. Tissue panels were probed using three different MLIP (1a, 1b and c, Figure 16) antibodies. When probing with MLIP 1b, we identified a MLIP variant at 46kDa in heart and skeletal muscle and a larger variant in the pancreas, weaker signals of different variants at sizes ranging from 25kDa – 200kDa (Figure 17 A and table 5). No major signals were noted in other tissue. On the other hand, when probing with MLIPc antibody, we noted a strong signal in the heart, but almost no signal in the skeletal muscle or other tissue. A weak band was present in the pancreas and a weak signal in the brain (Figure 17 B). Finally, probing with MLIP 1a gave several signals in various tissues, with the 46kDa band present only in heart, skeletal muscle and brain. MLIP protein expression profile is distributed differently in tissue (Figure 17 C).

As well, we probed for PKM2, LMNA and LMO7, which have been shown previously to interact with MLIP (Figure 6). When probing with PKM2, we identified very weak signals of PKM2 in thymus, spleen and the brain at 58kDa, likely due to the fact that PKM2 is expressed in early stages of development and in tissue with high ATP consumption (Christofk *et al* 2008) (Figure 17 D). Following that, we probed with a Lamin A/C (N-18) antibody and identified strong signals of Lamin C in both the heart and spleen and less stronger signals were found in the skeletal muscle, brain and liver (Figure 17 E) whereas Lamin A was only expressed in the heart, skeletal muscle and spleen with a very weak signal (Figure 17 E). Finally, probing with LMO7c antibody showed signals in the heart (90kDa), Skeletal muscle (110 kDa), spleen (46kDa) and the pancreas (30 kDa) (Figure 17 F). We recognized

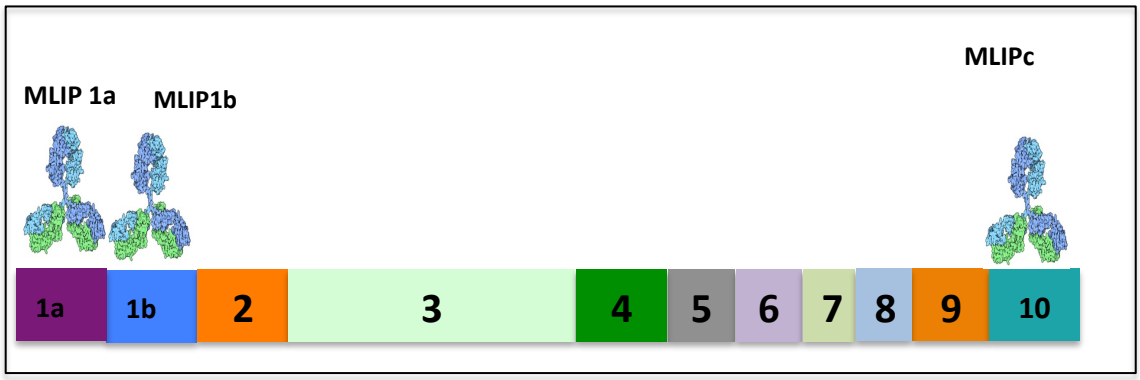

Figure 16 :Diagram of the MLIP antibodies. There are three MLIP antibodies that have been developed; MLIP-1a is directed against an epitope encoded within exon 1a. MLIP-1b is directed against an epitope encoded by exon 1b. MLIPc is directed against an epitope located on exon 10.

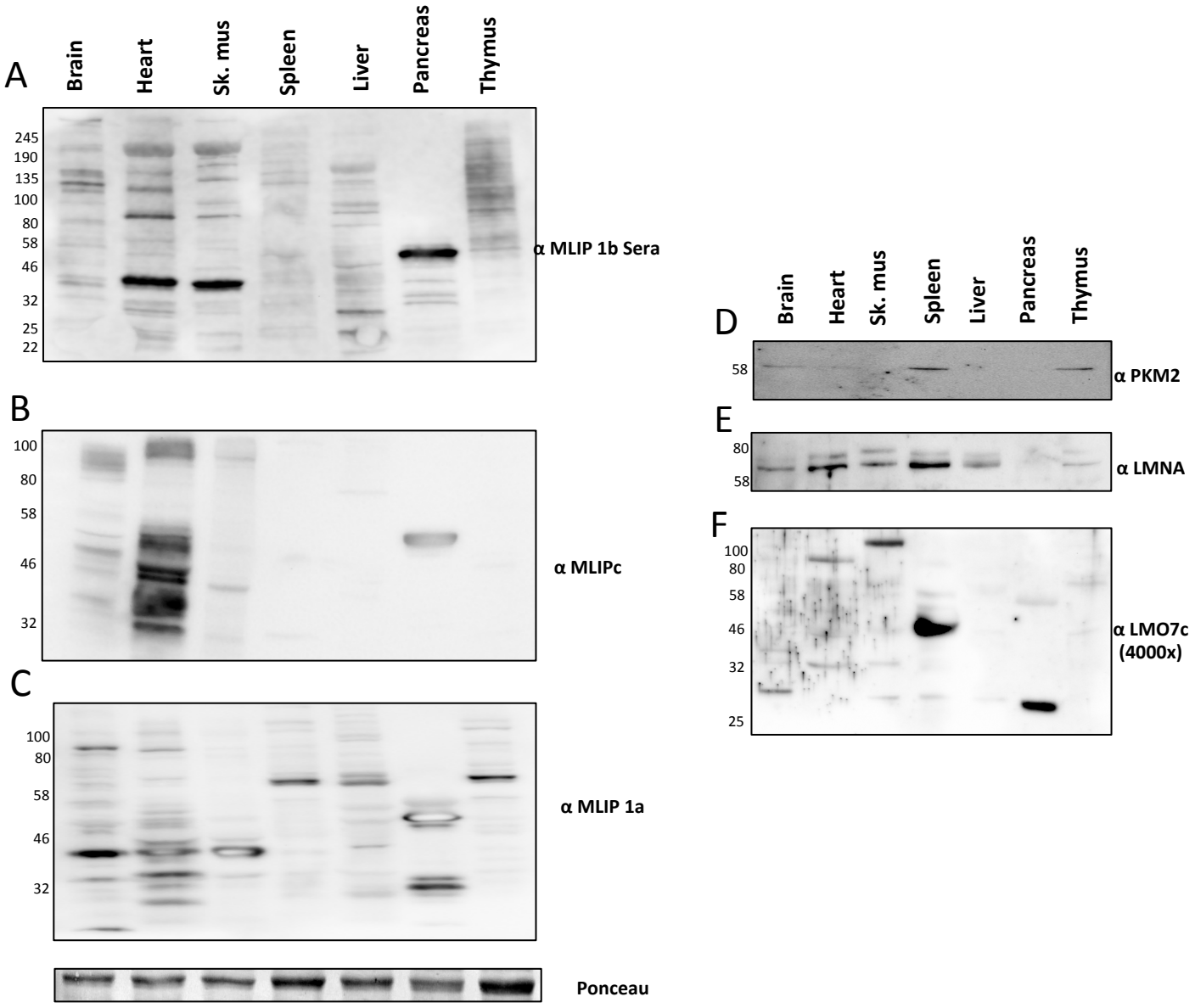

<u>Figure 17</u>: Endogenous Tissue distribution of mMLIP Profile. Tissue panels of adult male tissue with total of 20ug protein per lane and blots were probed with MLIP 1b (1:5000), MLIPc (1:5000), MLIP 1a (1:1000), PKM2 (1:1000), LMNA N-18 (1:1000) and LMO7c (Generous gift from James Holaska).

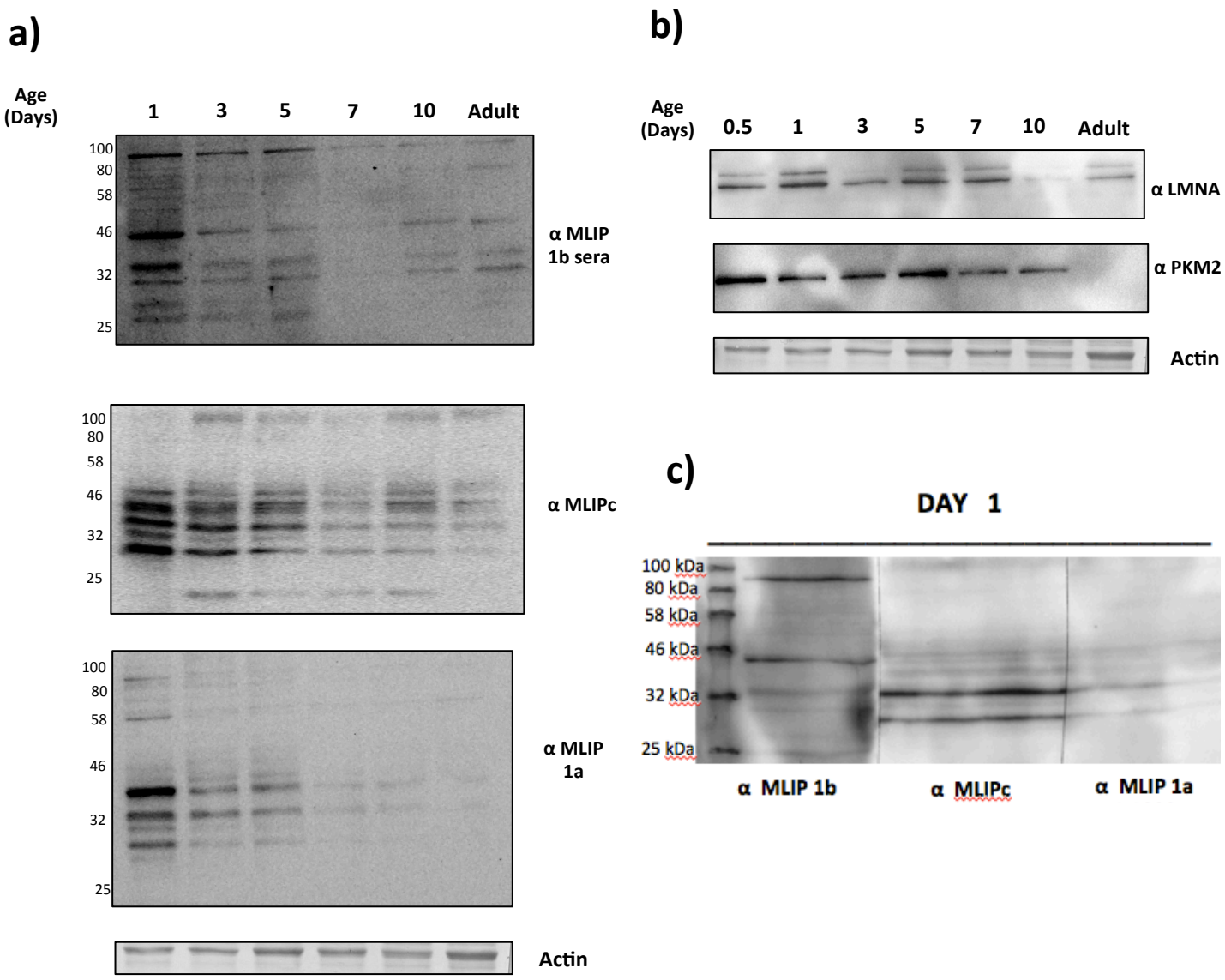

Figure 18: Endogenous Perinatal Heart distribution of mMLIP. Western blot analysis on Day 0.5, 1, 3, 5, 7, 10 and adult male hearts with total of 15ug/lane and blots were probed with MLIP 1b (1:5000), MLIPc (1:5000), MLIP 1a (1:1000), PKM2 (1:1000) and LMNA N-18 (1:1000).

an overlap in expression of MLIP and its splice variants in the tissue with the partners that resulted from the yeast two hybrid, giving more proof of the presence of the interactions.

Assessment of MLIP in postnatal hearts (Day 0.5, 1, 3, 5, 7, 10 and adult) heart showed a strong expression of MLIP and its splice variants at the early neonatal stages, which decreased as the mice aged. The pattern was consistent regardless of which MLIP antibody was used (1a, 1b or c) (Figure 18 a). As well, we probed for LMNA and PKM2. When probing for PKM2 we recognize the decrease in the level of expression as the mouse gets older and disappears at the adult stage. This suggests that MLIP plays a crucial role in post-natal heart development.

A summary of the expression profile of mMLIP 1b in each tissue is included in Table 5.

Table 5: Tissue distribution of endogenous mouse MLIP 1b variants, with their molecular sizes (Green = presence and Black = absence).

Isoform size	Brain	Heart	Skeletal Muscle	Spleen	Liver	Pancreas	Thymus
25 kDa							
30 kDa							
32 kDa							
34 kDa							
28 kDa							
40kDa							
42 kDa							
47 kDa							
52 kDa							
57 kDa							
59 kDa							
66 kDa							
81 kDa							
88 kDa							
90 kDa							
97 kDa							
100 kDa							
115 kDa							
129 kDa							
130 kDa							
145 kDa							
200 kDa							

7.5 Mouse MLIP is Alternatively Spliced Gene

Total heart and brain RNA was extracted and reverse transcription into cDNA was performed to identify MLIP splice variants that are encoded by exon 1a or 1b and tissue specificity. cDNA was amplified with primers designed to the 5' end exon 1b and exon 1a and amplifying the 3' end PCR anchor and E9-10 reverse (Figure 19 c). PCR products were confirmed by analysis on a 1% agarose gel stained with ethidium bromide. The primers 1a/E9-10 reverse and 1b/E9-10 reverse amplified in heart cDNA appear to have multiple bands, the primers 1a/PCR anchor and 1b/PCR anchor show multiple bands in the heart and brain. The results suggest that MLIP consists of multiple splice variants in both mouse heart and brain that are MLIP 1a and 1b specific (Figure 19).

To elucidate the protein expression profile of MLIP-1a and 1b, male adult heart and brain lysates were prepared for western blot analysis, probed with MLIPc and MLIP-1b and mRNA compared to protein expression. When we probed with MLIPc antibody we detected signals in both heart and brain. In the heart we identified multiple MLIP splice variants ranging in size between 28kDa-48kDa(28 kDa, 30kDa, 36kDa, 38kDa, 40kDa, 42kDa and 48kDa), whereas in the brain we detected a strong signal at 23kDa and other bands at 30kDa, 32kDa, 45kDa and 47kDa (Figure 19 b). When we probed with MLIP 1b we detect signals in both heart and brain. In the heart we detect strong band at 44kDa and weaker signals ranging 33kDa – 25kDa. Whereas the brain we detect multiple bands ranging between 46kDa-23kDa. Based on the resulted showed in both PCR and western blot analysis (green, blue and red

boxes) suggest that MLIP mRNA expression correlates directly with protein expression profile in mouse heart and brain (Figure 19 a).

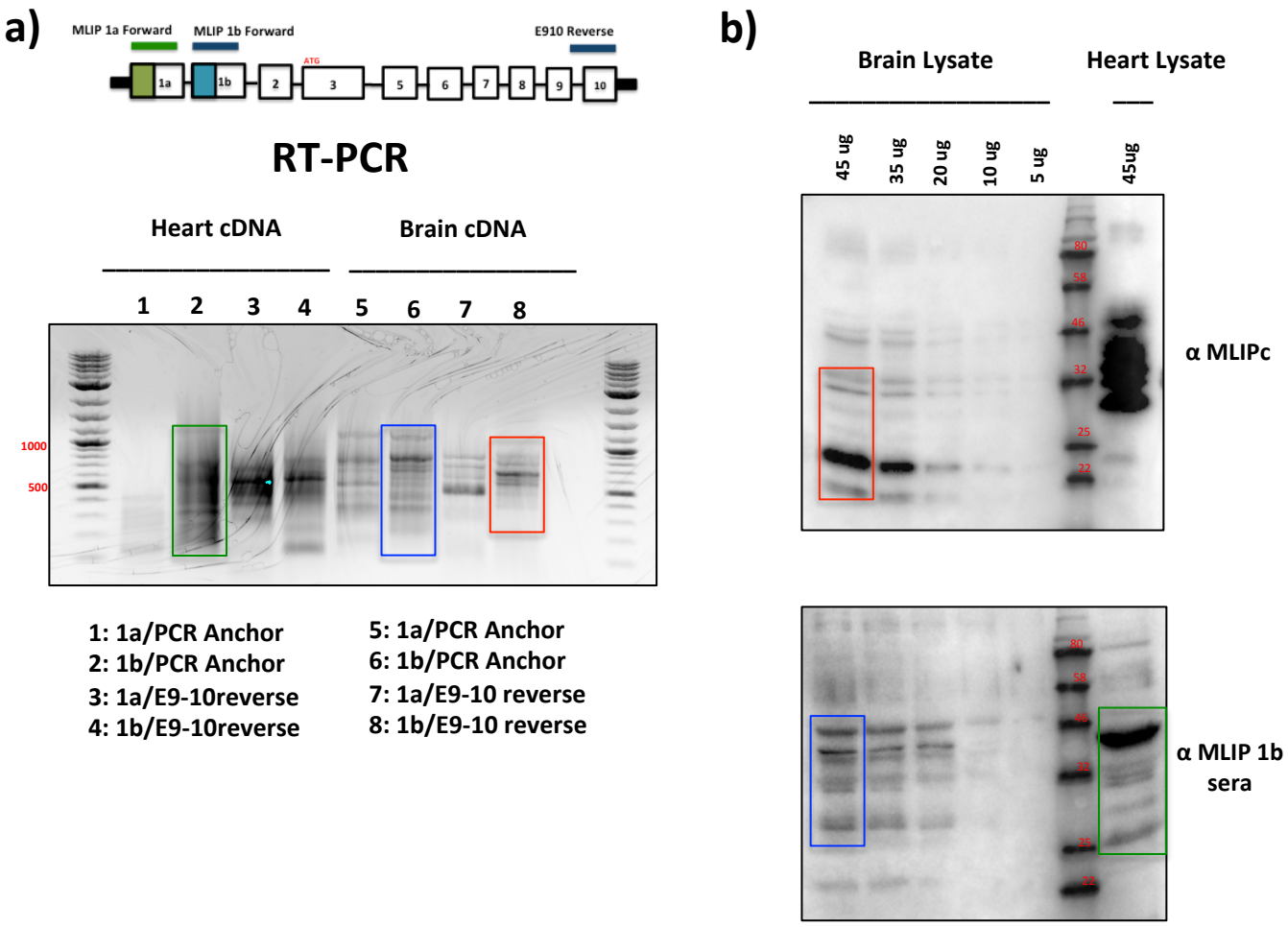

Figure 19: mMLIP alternatively Spliced Gene: a) RT-PCR was performed on mRNA isolated from mouse hearts and brains using primers to reverse transcribe the isolated mRNA and used primers to amplify exon 1a and 1b (5' end) and exon 9, 10 and poly A tail of MLIP to identify the MLIP 1a and 1b mRNA expression. b) Adult Brain tissue lysates were loaded at different concentrations starting 45ug, 35ug, 20ug 10ug and 5ug where as 45ug of heart lysate was loaded and detected via SDS PAGE electrophoresis and probed with Anti-MLIPc (1:5000) and Anti-MLIP 1b sera (1:5000).**The red, blue and green boxes highlighting MLIP mRNA and protein expression correlated directly in mouse heart .**

Chapter 4: Discussion, Conclusion & Future Directions

Discussion:

The novel gene, Muscle enriched A-type lamin Interacting protein (MLIP), was discovered by our lab through a yeast two-hybrid screening of human heart ventricular cDNA library approach using the first 230 amino acids of the LMNA gene as bait. We identified that the Lamin binding domain lies within the first 41 amino acids of MLIP (Figure 7) (Ahmady *et al* 2012).

In this project, we were able to demonstrate the presence of a novel hMLIP alternative start site in exon 3 (Figure 10) as well as an alternative promoter, MLIP 1b (Figure 12 b). We were also able to pinpoint the MLIP-Lamin A/C binding domain, which we discovered is exclusively specific to the protein encoded in exon-1a of hMLIP (Figure 15). Our data also reveals that MLIP undergoes tissue specific alternative splicing. MLIP is most abundantly expressed in the early stages of postnatal heart development (Figure 17 and 18). In addition, we confirmed that MLIP's isoforms gene expression and protein expression correlate directly in mouse heart (Figure 19).

Alternate Promoters:

Mammals have remarkably complex genomes; mammalian genes often produce multiple mRNA and protein isoforms composed by alternative processing of pre-mature RNA transcripts that may differ in structure, function and localization. Alternative processing has been identified to affect more than half of all human genes. One study by Kim *et al.* identified 10567 active promoters corresponding to 6763 known genes in human fibroblast cells, using high-density DNA microarrays.

In their analysis, they revealed that 1609 genes, representing 24% of total human fibroblast DNA, contain active multiple promoters (Kim *et al*. 2005). The *MLIP* gene is not alone in using alternative promoters, and there are several ways by which these promoters appear in genes (Figure 20) by gradual mutations, duplication of an existing promoter, insertion of a transposable element into the promoter region of the gene or genomic rearrangement resulting in insertion of an existing promoter in the ‘5 UTR gene region. The function behind the MLIP alternative promoters is not yet known but generally alternative promoters have different tissue specificity, developmental activity and/or expression level. Our data shows that MLIP gene has alternative promoters and a wide variation in protein isoform expression. The presence of alternative gene promoters can drive widespread cell type, tissue type or developmental gene regulation (Pajaares, M.J. *et al*. 2007). We believe that the combination of alternative promoters and start sites in MLIP gene results in an added complexity of MLIP gene regulation and leads to generation of multiple mRNAs, which encode different protein isoforms. The end result is a diverse and numerous amount of MLIP isoforms having a plethora of function, unique tissue distribution and possibly unique partners depending on cell type or tissue type studied.

MLIP:Lamin A/C Binding Domain

As part of these studies, characterization of the novel single copy gene MLIP was determined using several molecular biology techniques. MLIP was originally

identified as an interactor of A-type Lamins with the intention of understanding the mechanisms of Laminopathies (Ahmadi *et al*., 2011) (Figure 4). Mutations in A-type

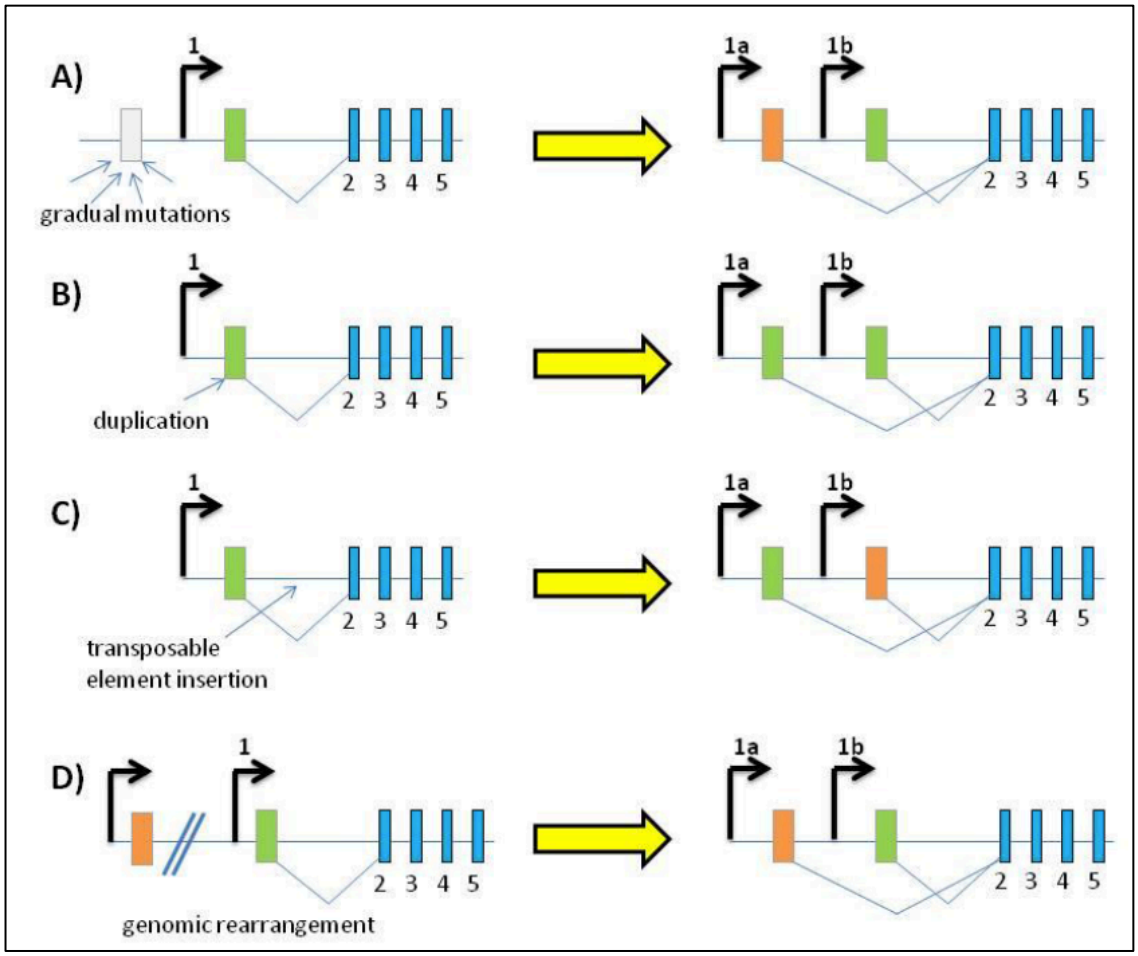

<u>Figure 20</u> : Schematic diagram demonstrating four possible origins of alternative promoters in a gene: A) by gradual mutation; B) by duplication of an existing promoter; C) by transposable element insertion and D) by genomic rearrangement and insertion of an existing promoter.

Lamins give rise to a wide spectrum of diseases affecting a wide range of tissues (Table 1), which mechanisms remain largely unknown. These mutations result in a heterogeneous group of disorders that affects specific combinations of tissue including the heart, skeletal muscle, neurons, and adipose tissue (Genschel J. 2000) (Figure 3). Bioinformatics analysis revealed that MLIP does not show any common ancestors; MLIP is shown to have a unique sequence and conserved gene among amniotes and is a heavily spliced gene. The yeast two hybrid by which MLIP was discovered displayed the MLIP:Lamin interaction to lie within the first 41 amino acids of the MLIP gene, this putative lamin binding domain spans across the protein encoded by exon 1 and exon 2 (Figure 7).

By means of immunoprecipitation and western blot analysis, it was clear to us that hMLIP binds to Lamin A/C *in-vitro* and this interaction is specific to the protein encoded by exon 1a (Figure 14) In addition, We performed *in-vivo* immune-precipitation to pull down lamin A/C and we were unable to prove the interaction because the IgG and Lamin A/C are both in the same size range and IgG signal was very strong that blocked Lamin A/C signal (data not shown). Furthermore, we confirmed that MLIP 1a is predominantly expressed in the heart and skeletal muscle (Figure 17), and MLIP's lamin A/C binding domain is exclusive to MLIP protein expressing 1a variant. Since heart and skeletal muscle predominantly express the 1a protein in MLIP suggests that the MLIP:Lamin A/C interaction takes place in these tissue and is of functional importance. It is also possible that mutations in this interaction can contribute to the pathogenesis of laminopathies.

MLIP, and interactors, tissue distribution

MLIP is ubiquitously expressed and is alternatively spliced in different tissue, with 7 known variants discovered (Δ2, Δ3, Δ4, Δ6, Δ8, Δ10 and Full length) (Figure 6). hMLIP consists of 10 exons and is flanked with 5' UTR, 3'UTR and alternative start site located on exon 3 (Figure 6B and 10). MLIP's expression differs in tissue and is subjected to extensive tissue dependent alternative splicing. The heart and skeletal muscle show a very similar expression patterns. Unique expression patterns in the thymus, pancreas and spleen suggest alternative functions in these tissues.

Previously identified interactors of MLIP, PKM2 and LMO7, tissue expression profile was investigated to elucidate the overlap of expression between MLIP splice variants and MLIP's interactors in order to identify potential physiological interaction. LMO7 is a LIM/homeodomain transcription factor that is alternatively spliced and is expressed in most tissue. LMO7 functions as a transcriptional activator through binding to Emerin and up-regulating its expression. Emerin is an integral inner nuclear membrane protein is required for maintaining nuclear envelope integrity and regulating heart specific gene expression (Dedeic *et al* 2011). Genome-wide association studies (GWAS) of genetic contributors to the pathogenesis of Type 1 Diabetes (T1D) examining ~2.54 million SNPs (Single Nucleotide Polymorphisms) in a combined cohort of 9,934 T1D and 16,956 controls, discovered three new loci associated with T1D. The most significantly associated SNP resides in an intronic region of the LMO7 gene (Bradfield J.P., 2011). LMO7 was found to be abundant in the pancreas along with

MLIP's multiple splice variants (Figure 17). This suggests that MLIP:LMO7 interaction could play a potential role in the pancreas and mutations in this interaction might play a role in Type 1 Diabetes.

Pyruvate kinase isozyme type M2 (PKM2) is a rate-controlling enzyme of the glycolytic pathway and catalyzes the formation of adenosine triphosphate (ATP) and pyruvate, which is consistently altered during tumorigenesis (Lee, Kim *et al*. 2008). PKM2 exists in both dimers and tetramers (Israelsen *et al*. 2013). The PKM2 isoform is found in the highly active tetrameric form, which favors ATP production through the tri-carboxylic acid (TCA) cycle, and the inactive dimeric form, which plays a vital role in aerobic glycolysis. Rapid depletion of substrate and oxygen can result in irreversible injury to the pre-served heart (Mazurek *et al*. 2005). A recent study (Shi *et al*. 2015) wanted to examine whether cardiomyocytes of heterotopic heart transplantation express PKM2 or not, and also if PKM2 regulates the apoptosis of cardiomyocytes after heart transplantation in rat. Data from that study demonstrated that PKM2 regulates the survival of cardiomyocytes after heterotopic heart transplantation in rat and that PKM2 may serve as a therapeutic target for protecting cardiomyocytes after heart transplantation. PKM2 was found to be highly expressed in the heart alongside MLIP, which points towards a potential role of MLIP:PKM2 interaction in the heart.

MLIP isoform gene and protein expression

Lamin A/C is expressed in the early stages of heart development (post-natal) starting from day 1 to 15. We noted a similar expression pattern for mMLIP in

the post-natal heart, showing high protein levels in the early days of heart development. mMLIP in day 1 heart tissue displays multiple splice variants specific to exon 1a and 1b (Figure 18 A and C), indicating that the MLIP-Lamin A/C interaction is functionally important for the early post-natal stages of heart development. The RT-PCR and western blot analysis demonstrate that mMLIP is heavily spliced protein with multiple splice variants that are exon 1a and 1b specific and elevated in male adult heart and brain as well as the mRNA expression correlated directly with MLIP protein expression profile.

Conclusion & Future Directions

Overall, the experiments conducted establish that hMLIP protein encoded by exon 1a specifically binds to Lamin A/C, which is predominantly expressed in skeletal muscle and cardiac tissue. Furthermore, during early stages of heart development, both MLIP and Lamin protein expression profiles are elevated. From this data, we believe that MLIPs interaction with Lamin A/C is crucial and any disruption in this interaction could possibly lead to diseases, contributing to Laminopathies.

We were also able identify the presence of alternative promoters in the MLIP gene that give rise to multiple splice variants, which are tissue and possibly cell unique. This analysis was accompanied by assessment of the other interactors LMO7 and PKM2, which showed unique tissue distribution as well. This confirms that MLIP gene processing is very complex and suggests that MLIP could play other roles depending on the tissue and the interacting partner.

There are many gaps in our understanding of MLIP's roles in pathways leading to muscle and cardiac differentiation and development of different muscular dystrophies seen in laminopathies. Additional research into exon-1a and 1b tissue specificity is needed before further conclusions can be drawn. Furthermore, studies to identify the exact location of the binding domain on Lamin A/C where MLIP 1a binds, followed by assessment of whether any of these sites are mutated in laminopathies will specifically link MLIP to laminopathies.

Finally, while there is a great deal of indicators pointing towards MLIP and the role it possess in both cardiac and smooth muscle function, MLIP appears to play a role in other tissues and possibly through other targets. Assessment of these interactions will help us better understand the exact function of MLIP.

Appendix

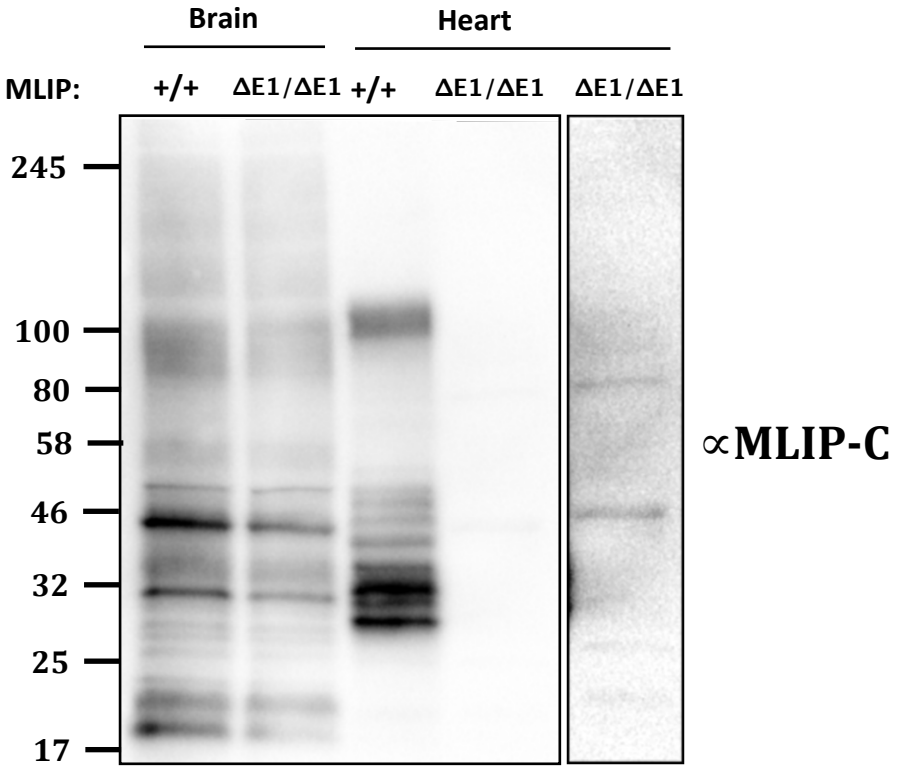

Figure 21 : Antibody Specificity. Mouse MLIP heart and brain lysates wild type and null heart and brain with a total of 40 ug per lane of protein and blot was probed with MLIPc antibody. Right hand panel longer exposure.

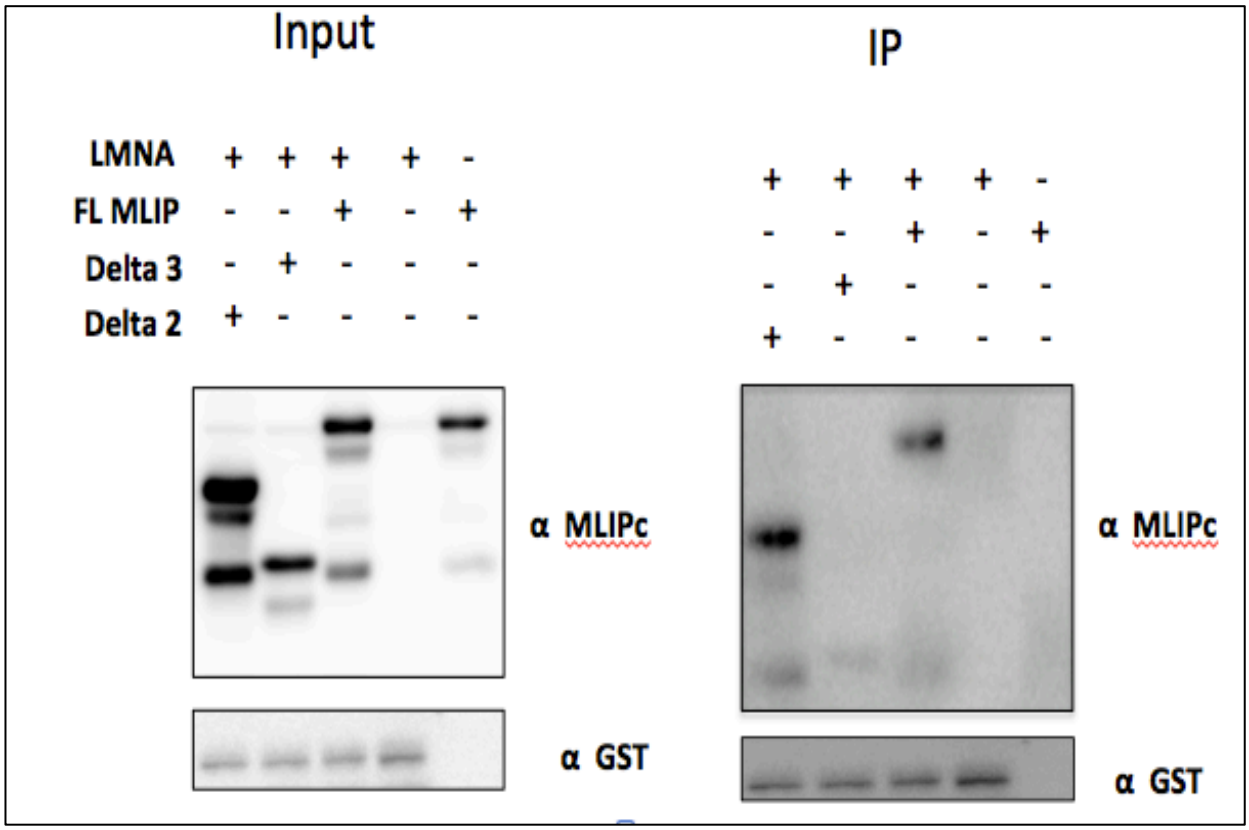

Figure 22: Purified recombinant GST-Lamin A/C binds directly with MLIP Specifically to the protein encoded by exon 1a in an in-vitro co-immunoprecipitation assay. Purified recombinant GST-Lamin A/C and TnT (Transcription Translation Systems) expressed MLIP isoforms were separately mixed together to form complexes precipitated through the Glutathione sepharose beads. Western analysis was performed using Anti-GST to determine the presence of lamin A/C in the pull down (1:1000) and Anti-MLIPc (1:5000) polyclonal antibodies to detect MLIP isoforms, this IP contains an additional control which we used full length MLIP to pull down with glutathione sepharose beads.

References:

- Stuurman N., Heins S., Aebi U. Nuclear lamins: their structure, assembly, and interactions. Journal of Structural Biology Volume 122, Issues1-2, 1998.

- ebi, U., Cohn, J., Buhle, L., and Gerace, L. (1986) The nuclear lamina is a meshwork of intermediate-type filaments, *Nature* **323,** 560–564.

- Hutchison J. C., Lamins: building blocks or regulators of gene expression? Nature 2002

- Bradfield, J. P., Qu, H.Q., Zhang, H., Sleiman, P. M., Kim,C. E., Mentch, F. D., Qiu, H., Glessner, J. T., Thomas, K. A., Frackelton, E. C., Chiavacci, R.M., Imielinski, M., Monos, D.S., Pandey, R., Bakay, M., Grant, S.F.A., Polychronakos, C., Kakonarson, H., (2011) A Genome-Wide Meta-Analysis of Six Type 1 Diabetes Cohorts Identifies Multiple Associated Loci, PLOS GENETICS, vol 7 issue 9.

- Genschel J, Schmidt HH. Mutations in the LMNA gene encoding lamin A/C. Human Mutation2000 Dec; 16(6):451-9.

- Quinlan RA, Schiller DL, Hatzfeld M, Achtstatter T, Moll R, Joranco JL, Magin TM, and Franke WW. Pastterns of expression and organization of cytokeratin intermediate filaments. Ann NY Acad Sci 455:282-306, 1985.

- Conway JF and Parry DA. Structural features in the heptad substructure and longer range repeats of two-stranded alpha-fibrous proteins. Int J Bio Macromol 12:328-334, 1990.

- Capell B.C. and Collins F.S. Human laminopathies: nuclei gone genetically awry. Nature 2006

- Broers JL, Ramaekers FC, Bonne G, Yaou RB, Hutchison CJ. Nuclear lamins: Laminopathies and their role in premature ageing. Physiology Review. 2006 jul:86(3):967-1008.
- Bertrand A., Chikhaoui K., Yaou R.B. and Bonne G. Clinical and Genetic Heterogenity in laminopathioes. Biochemicals transactions 2011.

- Röber RA, Weber K, Osborn M. Differential timing of nuclear lamin A/C expression in the various organs of the mouse embryo and the young animal: a developmental

study. Development. 1989 Feb;105(2):365-78

- Moir, R. D., Spann, T. P., Herrmann, H., & Goldman, R. D. (2000). Disruption of nuclear 104 lamin organization blocks the elongation phase of DNA replication. *Journal of Cell Biology, 149*(6), 1179-1191.

- Machiels BM, Zorenc AH, Endert JM, Kuijpers HJ, van Eys GJ, Ramaekers FC, Broers JL. An alternative splicing product of the lamin A/C gene lacks exon 10. Journal of Biological Chemistry 1996 Apr. 19; 271 (16) :9249-53.

- Zastrow MS, Vicek S, Wilson KL. Proteins that bind A-type lamins: integrating isolated clues. Journal of Cell Science. 2004 Mar 1;117(Pt7):979-87.

- Capell BC, Olive M, Erdos MR, Cao K, Faddah DA, Tavarez UL, Conneely KN, QU X, San H, Ganesh SK, Chen X, Avallone H, Kolodgie FD, Virmani R, Nabel EG and Collins FS. A farnesyltransferase inhibitor prevents both the onset and late progression of cardiovascular disease in a progeria mouse model. CrossMark vol. 105 no. 41; 15902-15907.

- Singla A, Griggs NW, Kwan R, Snider NT, Maitra D, Ernst SA, Herrmann H, Omary MB. Lamin aggregation is an early sensor of porphyria-induced liver injury. Journal Cell Science 2013 Jul 15; 126(14): 3105-3112.

- Meshorer E, Gruenbaum Y. Gone with the Wnt/Notch: stem cells in laminopathies, progeria, and aging. Journal of Cell Biology 2008 Apr 7; 181(1):9-13.

- Capell BC, Collins FS. Human laminopathies: nuclei gone genetically awry. Nature Reviews Genetics 7, 940-952 (December 2006).

- Ahmady E, Deeke SA, Rabaa S, Kouri L, Kenney L, Stewart AFR, Burgon PG. Identification of a Novel Muscle A-type Lamin-interacting Protein (MLIP). The Journal of Biological Chemistry, 286, 19702-19713.

- Murray-Zmijewski, F.*et al*. (2006) p53/p63/p73 isoforms: anorchestra of isoforms to harmonise cell differentiation and response to stress. Cell Death Differ. 13, 962-972.

- Christofk R. H., Vander Heiden G.M., Harris H.M., Ramanathan A., Gerszten E.R., Wei R., Fleming D.M., Schreiber L.S. and Cantley C. L. The M2 splice isoforms of pyruvate

kinase is important for cancer metabolism and tumor growth. Nature 452, 230-233 (13 March 2008).

- Torik A.Y., Ayoubi and Wim J. M., Van De Ven. (1998) Regulation of gene expression by alternative promoters. The FASEB Journal

- Kim H.T., Barrera O.L., Zheng M., Qu C., Singer A.M., Richmond A.T., Wu Y., Green D.R., and Ren B., A high-resolution map of active promoters in the human genome. Nature 436, 876-880 (2005).

- Dedeic Z., Cetera M., Cohen V. T. and Holaska M. J., Emerin inhibits LMO7 binding to the Pax3 and MyoD promoters and expression of myoblast proliferation genes. Cell Science 2011.

- Ben Yaou, R., *et al*., Genetics of laminopathies. Novartis Found Symp, 2005. 264: p. 81-90;
discussion 90-97, 227-30.

- Charniot, J.C., *et al*., Functional consequences of an LMNA mutation associated with a new cardiac and non-cardiac phenotype.

- Novelli G., *et al*., Mandibuloacral dysplasia is caused by mutations in LMNA-encoding Lamin A/C. Am J Hum Genet, 2002. 71(2): p.426-31.

- Muchir, A., *et al*., Identification of mutations in the gene encoding lamins A/C in autosomal dominant limb girdle muscular dystrophy with atrioventricular conduction disturbances (LGMD1B). Hum Mol Genet, 2000. 9(9): p. 1453-9.

- Taylor, M.R., *et al*., Natural history of dilated cardiomyopathy due to lamin A/C gene mutations. J Am Coll Cardiol, 2003. 41(5): p. 771-80.

- Bonne, G., *et al*., Clinical and molecular genetic spectrum of autosomal dominant Emery-
Dreifuss muscular dystrophy due to mutations of the lamin A/C gene. Ann Neurol, 2000. 48(2): p. 170-80.

- Brodsky, G.L., *et al*., Lamin A/C gene mutation associated with dilated cardiomyopathy with variable skeletal muscle involvement. Circulation, 2000. 101(5): p. 473-6.

- Bonne, G., *et al*., Mutations in the gene encoding lamin A/C cause autosomal dominant Emery-Dreifuss muscular dystrophy. Nat Genet, 1999. 21(3): p. 285-8.

- Kitaguchi, T., *et al*., A missense mutation in the exon 8 of lamin A/C gene in a Japanese case of autosomal dominant limb-girdle muscular dystrophy and cardiac conduction block. Neuromuscul Disord, 2001. 11(6-7): p. 542-6.

- Hong, J.S., *et al*., Cardiac dysrhythmias, cardiomyopathy and muscular dystrophy in patients
  with Emery-Dreifuss muscular dystrophy and limb-girdle muscular dystrophy type 1B. J Korean Med Sci, 2005. 20(2): p. 283-90.

- Becane, H.M., *et al*., High incidence of sudden death with conduction system and myocardial disease due to lamins A and C gene mutation. Pacing Clin Electrophysiol, 2000. 23(11 Pt 1): p.1661-6.

- Brown, C.A., *et al*., Novel and recurrent mutations in lamin A/C in patients with Emery-Dreifuss muscular dystrophy. Am J Med Genet, 2001. 102(4): p. 359-67.

- Emery, A.E., Emery-Dreifuss syndrome. J Med Genet, 1989. 26(10): p. 637-41.

- Sullivan, T., *et al*., Loss of A-type lamin expression compromises nuclear envelope integrity leading to muscular dystrophy. J Cell Biol, 1999. 147(5): p. 913-20.

- Pajares, M.J. *et al*. (2007) Alternative splicing: an emerging topic in molecular and clinical oncology. Lancet Oncol. 8, 349–357.

- Lee J., Kim H.K., Han Y., Kim J. Pyruvate kinase isozyme type M2 (interacts) and cooperates with Oct-4 in regulating transcription. IJBCB 40 1043-1054 (2008).

- Israelsen J.W., Dayton L.T., Davidson M.S., Fiske P.B., Hosios M.A., Bellinger G, Li J., Yu Y., Sasaki M., Homer W.J., Xie J., Jurczak J. M., DePinho A.R., Cantley C.L., and Vander Heiden G.M. PKM2 isoform-specific deletion reveals a differential requirement for pyruvate kinase in tumor cells. Cell 155, 397-409 (2013)

- Shi J., Yang X., Yang D., Li Y., Liu Y. Pyruvate kinase isozyme M2 expression correlates with survival of cardiomyocytes after allogeneic rat heterotopic heart transplantation. Pathology- research and practice volume 211, issue 1, 2015.

- Cattin, M.E., Wang,J., Weldrick,J. Roeske, C. Mak, E. Thorn,S. Deletion of Muscle-enriched A-type Lamin-Interacting Protein (MLIP) leads to Cardiac Hyperactivation of Akt/mTOR and Impaired Cardiac Adaptation. Journal of Biological Chemistry. September 2015.